



An energy-efficient cyclic amine system developed for carbon capture from both flue gas and air



Guanchu Lu^a, Zongyang Yue^a, Yanan Deng^a, Yuxiang Xue^a, Yi Huang^a, Xiaolei Zhang^b, Xianfeng Chen^a, Xianfeng Fan^{a,*}

^a Institute for Materials and Processes, School of Engineering, the University of Edinburgh, Edinburgh EH9 3FB, Scotland, UK

^b Chemical and Process Engineering, University of Strathclyde, Glasgow G1 1XQ, Scotland, UK

ARTICLE INFO

Keywords:

Non-aqueous CO₂ absorbents
Post-combustion capture
Low energy regeneration
DFT calculation
Direct air capture

ABSTRACT

High energy consumption is a major barrier to the large-scale deployment of carbon capture processes from flue gases or air (direct air capture, DAC). The non-aqueous amines reported in literature possess a high energy efficiency for CO₂ capture from flue gases, they struggle with gas streams containing ultra-dilute CO₂, like air, due to poor absorption kinetics. This study developed novel 2-PE (2-piperidineethanol)/APZ (Aminoethylpiperazine) based CO₂ absorbents to address these problems. The experiments and MD simulation results showed that the 2-PE/APZ-based absorbents possessed a superior absorption performance both in flue gas and air. Among the developed absorbents, when 2-PE/APZ mixed with DMF (Dimethylformamide), the CO₂ loading reached to 1.004 mol/mole, as the theoretical maximum. In DAC tests, 87.31 % CO₂ from the air was captured in 24 h experiments. The regeneration heat duty of 2-PE/APZ/DMF decreased to 1.694 KJ/g CO₂, a 55.89 % reduction compared to the benchmark 30 wt% MEA. The CO₂ absorption/desorption mechanism was analysed by NMR, In-situ FT-IR, and DFT calculation. It indicated that this significant improvement in CO₂ absorption performance and the reduction in energy consumption are due to the synergistic effect of 2-PE and APZ. During CO₂ absorption, CO₂ reacts with APZ forming APZ zwitterion rapidly, then deprotonation to the 2-PE. The formation of protonated 2-PEH⁺ ion pairs with APZCOO⁻ reduces hydrogen bonds and van der Waals forces among the amine-CO₂ complex, facilitating easy regeneration at mild conditions while maintaining high reactivity. The combination of theoretical and experimental results indicates that 2-PE/APZ-based absorbents can serve as a promising alternative for carbon capture from flue gas to air with low energy usage.

1. Introduction

Developing a sustainable society demands a concerted effort to combat rising atmospheric carbon dioxide (CO₂) levels, a critical driver of global warming and climate change [1]. Reducing CO₂ levels requires a combined effort to limit future emissions and develop strategies for decreasing existing concentrations. Anthropogenic CO₂ emissions have been identified as a primary cause of the increase in average global temperature due to greenhouse effects. Nowadays, most developed carbon capture technologies focus on CO₂ capture from industrial installations and power plants. A complementary approach to carbon capture is to capture CO₂ directly from the air, known as direct air capture (DAC). DAC has the advantage of location flexibility, and the input gas stream and ambient air are relatively clean, as the concentrations of SO_x and NO_x are low. However, DAC has the disadvantage of

having a dilute input stream, with air today containing about 450 ppm of CO₂. This necessitates the need for a high-capacity absorbent that is suitable for both high-concentration and low-concentration CO₂ capture with low energy usage [2].

Among the prevalent methodologies, traditional amine capture stands out as a prominent technique for handling higher-concentration CO₂ emissions, commonly found in flue gases from industrial processes [3]. However, this method bears a substantial energy penalty, notably when addressing lower concentrations of CO₂, typically below 1 % [4]. The energy-intensive nature of traditional amine capture has led researchers to explore alternative avenues for CO₂ capture, sparking interest in non-aqueous absorbents based on organic amine solutions [5]. Currently, the most-well-established sorbent, monoethanolamine (MEA), requires a temperature of > 393 K for efficient CO₂ desorption, and the regeneration energy of aqueous MEA absorbents ranges from 3.9–4.5 MJ/KG CO₂, heat duty for solvent regeneration can constitute up

* Corresponding author.

E-mail address: x.fan@ed.ac.uk (X. Fan).

Nomenclature

r_{abs}	Absorption rate of CO ₂ (g-CO ₂ / (kg-soln. ·min.)),
r_{des}	Desorption rate of CO ₂ (g-CO ₂ / (kg-soln. ·min.)),
r_{CO_2input}	The input absorption rate of CO ₂ (g-CO ₂ / (kg-soln. ·min.)),
a_{CO_2rich}	CO ₂ capacity in the CO ₂ -rich liquid (g-CO ₂ /kg-soln.).
a_{CO_2poor}	CO ₂ capacity in the CO ₂ -lean liquid (g-CO ₂ /kg-soln.).
ΔG_{sol}	Solvation free energy (KJ/mole).
η_{abs} CO ₂	Absorption rate efficiency (%)
η_{des} CO ₂	Desorption efficiency (%)
Q	Regeneration energy (KJ/g)
Q_s	Sensible heat (KJ/g)
Q_r	Reaction heat of desorption (KJ/g)
Q_v	Latent heat of vaporization (KJ/g)
EC	Ratio of energy/released CO ₂ (KJ/mole),
C_p	Specific heat capacity (KJ/mol · K ⁻¹),

to 70 % of the total operating costs in a CO₂ capture plant, leading to operational challenges and equipment corrosion [6]. The realm of non-aqueous absorbents presents an evolving landscape, leveraging the synergistic potential of amine and solvent components. Organic solvents ranging from alcohols [7–9], glycols [10–14], glycol ethers [15–18], glymes [19], pyrrolidones [20,21], and formamides [22,23] have emerged as promising candidates, offering distinct advantages over aqueous solutions. By replacing the solvent from water with organic solvents, energy consumption could be reduced by 20 % to 60 %, varying from 2.0 to 2.9 KJ/g CO₂, based on solvent choice [24,25].

While amine capture has predominantly been employed in post-combustion capture processes (PCC) handling concentrations of 8–16 %, expanding its application to capture CO₂ from sources such as enclosed spaces (e.g., submarines and space stations with 1 % CO₂) or direct capture from ambient air (at 450 ppm CO₂) remains a technological frontier [4]. This expansion, particularly in the realm of DAC, presents a pathway to reduce carbon capture costs. However, the efficiency of current non-aqueous absorbents in capturing super-dilute CO₂ streams remains a bottleneck [26]. Although these absorbents reduce vapor losses, their sluggish CO₂ absorption capabilities hinder the efficiency of DAC processes. Meanwhile, the efficacy of non-aqueous absorbents, in contrast to their aqueous counterparts, reveals a notable performance discrepancy. Barzaghi et al. compared CO₂ capture performance of various amines including MEA, DEA, and AMP with water and DEGMEE. While amine-DEGMEE hold lower energy penalty, they exhibited inferior CO₂ absorption rate and capacity [27]. These studies underscore the criticality of solvent selection for non-aqueous absorbents, emphasizing the current reliance on extensive experimental testing. Given this reliance, the academic community urgently seeks a straightforward and dependable screening method to enhance solvent selection processes. Based on this screening method, the researchers could quickly screen different solvents and develop an ideal non-aqueous absorbent, which could capture CO₂ from various CO₂ concentration streams, regenerate at lower temperatures, be resilient for enduring multiple CO₂ absorption–desorption cycles, and most important, relatively low energy penalty during desorption.

The current research of non-aqueous absorbents focuses on primary and secondary amines with organic solvents [28]; Notably, research on cyclic amines is relatively scarce, and within this context, 2-piperidineethanol (2-PE) stands out as a cyclic sterically hindered amine (SHA). While 2-PE has been previously investigated for CO₂ absorption, its low absorption efficiency has constrained the broader application [29]. Another cyclic amine, aminoethylpiperazine (APZ), distinguished by its three amino groups, possesses high reactivity with CO₂. However, the non-aqueous APZ absorbents leads to precipitation during CO₂

absorption process, suspending the continuous CO₂ capture. By combining 2-PE and APZ, adjusting their concentration ratio, and identifying appropriate solvents, the 2-PE/APZ absorbents could capture CO₂ from both flue gas and air with great absorption performance and low energy consumption simultaneously.

In this study, the 2-PE/APZ-based absorbents were developed using a solvent screening strategy via molecular dynamics (MD) simulation and density functional theory (DFT) calculation. This innovative approach builds upon our prior research and demonstrates the use of different solvents to influence CO₂ capture performance, the subsequent absorption experiments also verified the validity of this method. In addition to the CO₂ capture from flue gas, the 2-PE/APZ-based absorbents also could effectively capture CO₂ from high flow-rate air. More than 96 % CO₂ from air was captured in the first 12 h of DAC experiments. The desorption efficiencies of 2-PE/APZ-based absorbents are also impressive, more than 90 % CO₂ was desorbed under 363 K. To understand the absorption/desorption mechanism of 2-PE/APZ-based absorbents, various analytical techniques, including nuclear magnetic resonance (NMR), Fourier-transform infrared spectroscopy (FT-IR), differential thermal calorimetry (DSC) and DFT calculation are utilized. The resulted showed that synergistic effect of 2-PE and APZ plays the critical role in their excellent absorption and desorption performance. The formation of 2-PEH⁺ and APZCOO⁻ ion pairs significantly weakened hydrogen bonds and van der Waals attraction among the CO₂ loaded amine system. This synergistic effect enables 2-PE/APZ-based absorbents to maintain the superior high reactivity of APZ and facilitates low-temperature regeneration ability, as well as prevents the precipitation of APZ zwitterion (APZH⁺COO⁻) and increased CO₂ absorption capacity of 191.8 % in comparison to single 2-PE absorbents. Overall, the developed 2-PE/APZ-based absorbents have the ability to capture CO₂ from both flue gas and air coupled with extremely low energy consumption, marking a significant advancement in CCS technologies.

2. Materials and experimental sections

2.1. Materials

In this work, all solutions were prepared by using 2-piperidineethanol (2-PE, purity ≥ 95 %, ACROS Organics), Aminoethylpiperazine (APZ, purity ≥ 99 %, MERCK LIFE), N, N-Dimethylformamide anhydrous (DMF, 98 %, purity ≥ 99 %, MERCK LIFE), Dimethyl sulfoxide (DMSO, 98 %, purity ≥ 99 %, MERCK LIFE), N-Methylformamide (NMF, 98 %, purity ≥ 99 %, MERCK LIFE), diethylene glycol monoethyl ether (DEGME, 99 %, Honeywell), ethylene glycol (EG, 99 %, Sigma-Aldrich UK), piperazine (PZ, 99 %, Fisher Chemical), Ethanolamine (MEA, purity ≥ 99 %, Sigma-Aldrich UK), 1-(2-Hydroxyethyl)piperazine (HPZ, 98 %, MERCK LIFE), 2-Methylpiperazine (MPZ, 98 %, Fisher Chemical). Gases used for absorption and desorption experiments (CO₂ and N₂) were of commercial grade with a minimum purity of 99.99 % (Linde Group UK).

2.2. Absorption and desorption setup and calculation method

As a detailed description of the absorption and desorption setup is presented in Fig.S1 and Fig.S2 [29–32].

2.3. Experimental procedures

The experimental work for evaluating the 2-PE/APZ-based absorbents is methodically segmented into four parts. The first part involves using MD simulation and DFT calculation to screen solvents mixed with 2-PE/APZ for effective CO₂ absorption. Following this, absorption experiments were conducted using various CO₂ sources—flue gas (20 v% CO₂), enclosed spaces (1 v% CO₂), and direct from air (450 ppm CO₂). Subsequently, the saturated absorbents are subjected to desorption processes at temperatures ranging from 323 K to 363 K. The third part

conducted cyclic experiments, thermal stability tests, and energy consumption calculations. The final part focuses on the absorption/desorption mechanism, combining various characterization methods and DFT calculation. To simplify the absorbent's name, the composition such as "30 % 2-PE/20 % APZ/DMF" is abbreviated as "2-PE/APZ/DMF (3-2)" in following section.

2.4. Characterization analysis

Characterization analysis in this research included DSC Analysis, in-situ ATR-FTIR, rheometer and NMR (^1H and ^{13}C). The experimental setup is available at [Supporting Information part 2](#).

2.5. MD simulation and DFT calculation

In this study, the MD simulation is conducted by Materials Studio 2020 (MS 2020) to research the solubility changes during various absorption stages [23,33]. The DFT calculation is divided into three main parts. The DFT study begins with calculating energy barriers and Gibbs free energy changes using the MS 2020 DMol3 modules [34]. The GGA/BLYP DNP 3.5 was taken as functional basic. Then, the calculation involves optimizing molecular configurations, harmonic frequencies, and energy changes of reactants, products, and transition states, which are performed at the B3LYP/6-311++G** level with DFT-D3 correction in the Gaussian 09 [35-37], focusing on detailed molecular insights. Finally, solvation free energies are determined using the M062X/6-31G* basis set in Gaussian 09, employing a universal solvation model (SMD) to understand solvent interactions [37]. Details are available in [Supporting Information Part 7](#).

2.6. Independent gradient model based on Hirshfeld partition (IGMH) analysis

To elucidate the desorption mechanism of 2-PE/APZ-based absorbents, an IGMH analysis was performed at Multiwgn programme [38,39]. This analysis, grounded in the Hirshfeld partitioning of molecular density, was employed to visually examine both intramolecular and intermolecular interactions within the 2-PEH⁺/APZCOO⁻ complex. Detailed methodology and setup can be found in the [Supporting Information Part 7](#).

3. Results and discussion

3.1. The solvent screening for 2-PE/APZ-based absorbents on MD simulation

To develop the non-aqueous amine CO₂ absorbents, solvent selection is crucial. The physicochemical properties of organic solvents, including heat capacity, viscosity, and dielectric constant, hold strong impact on the CO₂ capture performance. Traditionally, solvent screening requires extensive experimental efforts [40]. In our previous research, a robust and expedient solvent screening strategy based on MD simulation has been developed. We constructed the amorphous cells containing 2-PE, APZ, and solvent molecules, and then calculated the average van der Waals (vdW) solubility parameters at different stages of absorption [34]. It is noteworthy that MD simulations conducted in this study differ from traditional CO₂ absorption MD simulations involving chemical reactions. Our simulations focused on non-reactive conditions at different stages of the reaction, where CO₂ was introduced into the simulation box in the form of carbamates/carbonates, thus bypassing direct chemical reactions between CO₂ molecules and amines. Instead, the simulations only encompassed the diffusion processes between amine-CO₂ products and organic solvent molecules. Under these circumstances, equilibrium could be achieved in a relatively short simulation time (10 ps) [34]. Through the interaction between solvent and solute molecules, the solubility parameters could be accurately calculated. Detailed

information can be found in [Supporting Information Part 7](#).

As seen from [Fig. 1\(a\)](#), five different solvents including DMF, DMSO, NMF, DEGMEE and EG were selected to mixed with 30 wt% 2-PE and 20 wt% APZ. These five organics could be categorised as aprotic solvents, ethers, and glycols, as commonly used solvents in non-aqueous CO₂ absorbents. The CO₂ reaction stage is quantified through CO₂ loading metrics, ranging from 0 to 1 (mole CO₂/mole amine), denoting the ratio of CO₂ molecules absorbed per mole of amine present. MD simulations were conducted across When the CO₂ loading is 0.1 (mole CO₂/mole amine), it means that 1/10 of the amine is reacted with CO₂ to form carbamate. It was observed that as CO₂ absorption advanced, the vdW solubility parameters diminished, ultimately stabilizing at a relative plateau. Specifically, for the 2-PE/APZ/DMSO (3-2) system, as shown in [Fig. 1\(a\)](#), the vdW solubility parameter decreased from 19.1888 at 0 CO₂ loading to 15.1269 at 0.9 CO₂ loading, thereafter maintaining a stable range around 15.3 until the CO₂ loading is 1.0 (mole CO₂/mole amine). This pattern indicates that the MD simulations effectively predict the CO₂ loading for 2-PE/APZ/DMSO (3-2) to be between 0.9 and 0.95 (mole CO₂/mole amine), which closely corresponds with our experimental findings (0.941) in next section. Therefore, this MD simulation methodology presents a promising avenue for the screening of solvents in the development CO₂ absorbents.

[Fig. 1\(a\)](#) delineates the influence of solvent choice on the solubility parameter trends for 2-PE/APZ-based absorbents, with the vdW solubility parameters showing a hierarchy of aprotic solvents > ethers > glycols. Among these solvents, EG exhibited the lowest vdW solubility, and it suggested the least efficient CO₂ capture performance when using EG as a solvent. The vdW solubility parameters for 2-PE/APZ in aprotic solvents (DMF, NMF, and DMSO) approximate 19.5, suggesting similar CO₂ capture ability across these solvents. As CO₂ loading increases, a decrease in vdW solubility is observed until equilibrium is attained; the solubility at this equilibrium point corresponds to the maximum absorption capacity as determined through experimental measures. In MD simulation, the prediction for the maximum CO₂ loading range of 2-PE/APZ/DMF was around 1.0, with similar findings for 2-PE/APZ/DMSO and 2-PE/APZ/NMF, both approximating 0.9. These predictions range closely matched experimental values in [Section 3.2](#); 1.004 (mole CO₂/mole amine) for 2-PE/APZ/DMF, 0.941 (mole CO₂/mole amine) for 2-PE/APZ/DMSO, and 0.911 (mole CO₂/mole amine) for 2-PE/APZ/NMF. Among the solvents studied, 2-PE/APZ/DMF demonstrated superior CO₂ capture efficiency, underscoring its potential as a preferred solvent in the formulation of effective CO₂ absorbents.

[Fig. 1\(b\)](#) explores the impact of varying APZ concentrations on the CO₂ capture performance of 2-PE/APZ/DMF absorbents, with the APZ concentration ranging from 5 wt% to 30 wt%. An increase in APZ concentration resulted in a decrease in vdW solubility, reflecting a diminished solubility attributed to the reduced solvent content. For these 2-PE/APZ/DMF absorbents, with CO₂ loading increased, the vdW solubility showed consistent trends, decreasing with rising CO₂ absorption loading until equilibrium is reached. Predictions of CO₂ uptake loads from MD simulations were in general agreement with experimental results presented in [Section 3.2](#). Nonetheless, at an APZ concentration of 30 wt%, the absorption content projected by MD simulations fell within the range of 0.95–1.0 (mole CO₂/mole amine). Contrarily, the experimentally determined absorption content was 0.892 (mole CO₂/mole amine), diverging from the anticipated range. This discrepancy can primarily be attributed to the solvent content being lower than that of the solute, which in turn weakened the solvation effect. Additionally, the reduction in DMF content not only diminished the solvent's efficacy but also escalated the viscosity of the absorbent mixture, adversely affecting its CO₂ absorption capability. This insight underscores the critical balance between solvent and solute concentrations in optimizing the CO₂ capture performance of such absorbent systems.

To elucidate the influence of solubility on the efficacy of non-aqueous CO₂ absorbents, solvation free energy (ΔG_{sol}) calculations were performed for various amine-CO₂ complexes [37], as depicted in

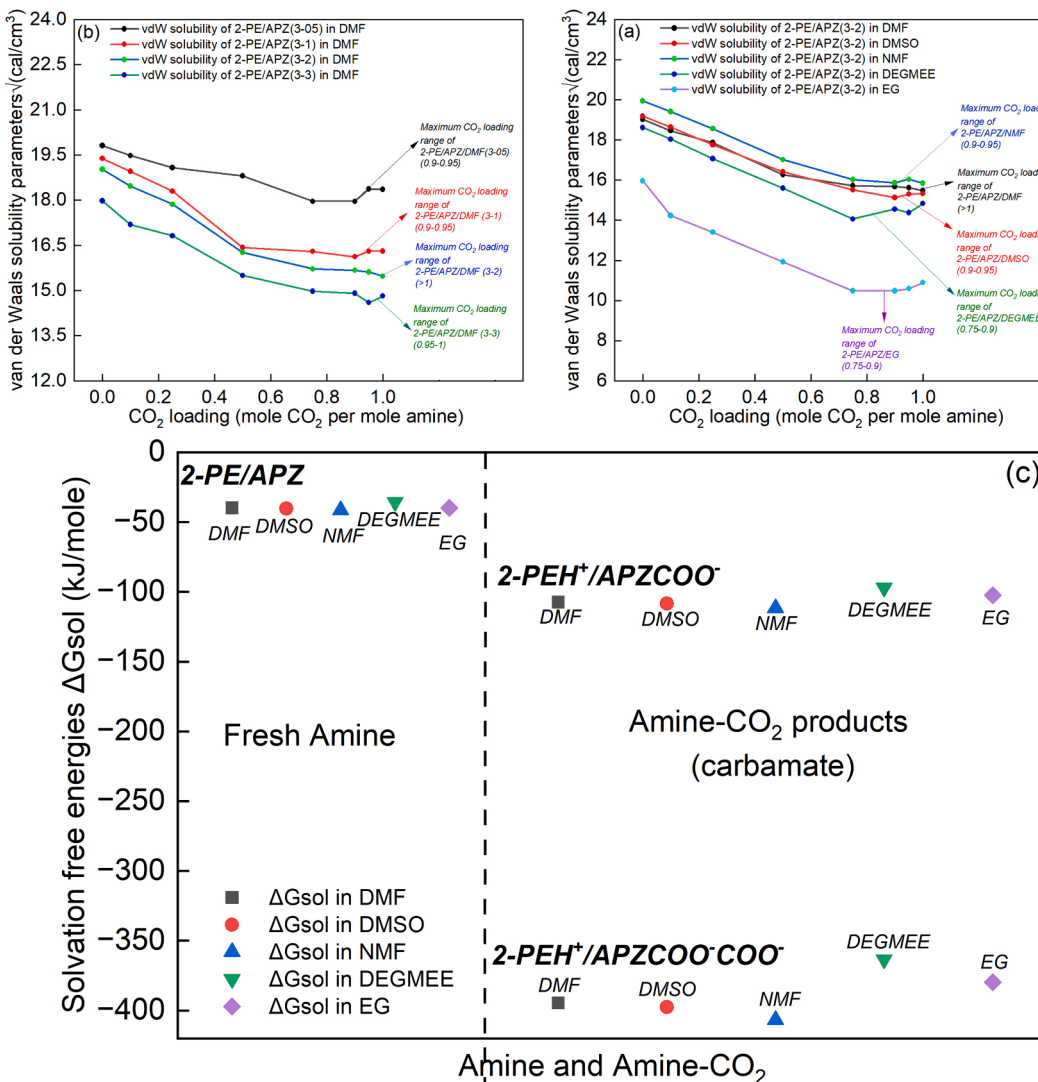


Fig. 1. The results of MD simulation and DFT calculation. a) vdW solubility parameters of 2-PE/APZ with DMF, DMSO, NMF, DEGMEE and EG at different CO₂ loading. b) vdW solubility of vdW solubility parameters of 2-PE/APZ. c) Solvation free energies of fresh amine(left) and amine-CO₂ products(right) of 2-PE/APZ in various solvents.

Fig. 1(c). The solvation free energy, alongside solubility parameters, serves as critical indicators of the solvation effect. ΔGsol represents the change in free energy accompanying the transition of a molecule from an ideal gas state to dissolution in a solvent, determined through DFT calculations with M062X basis set. Without accounting for the free energies of evaporation, the solvation free energies offer insights into solubility trends, with lower ΔGsol values indicative of higher solubility.

In the context of 2-PE/APZ-based absorbents, the solvation free energy calculations with various solvents elucidate the observed disparities in solubility. The left side of Fig. 1(c) presents the solvation free energies for unreacted amine in solvents including DMF, DMSO, NMF, DEGMEE, and EG, with ΔGsol values ranging from -35.65 to -41.53 kJ/mole. This indicates comparable solubility levels of the unreacted 2-PE/APZ across these organic solvents. Conversely, the right side of Fig. 1(c) details the solvation free energies for CO₂-loaded amine. According to NMR spectra, 2-PEH⁺/APZCOO⁻ is identified as the predominant initial reaction product, exhibiting minor variations in solvation free energies across different solvents, from -97.12 to -111.46 kJ/mole. This suggests that the initial CO₂ reaction products are well solubilized in these selected solvents, agreeing well with CO₂ absorption experiments in Section 3.2.

With CO₂ absorption progresses, the primary CO₂ reaction product

transitions from 2-PEH⁺/APZCOO⁻ to 2-PEH⁺/APZ(COO⁻)₂, reflecting the consumption of primary amine reactive sites in APZ. The solvation free energies for this product demonstrate a preference hierarchy: DMF, DMSO, NMF > DEGMEE > EG. This hierarchy indicates that differences in CO₂ absorption efficiency resulting from solvent selection are largely due to the varied solubility of 2-PEH⁺/APZ(COO⁻)₂, in which EG exhibits the lowest solubility, and consequently the weakest CO₂ capture capacity. These insights guide the formulation of subsequent experimental designs to validate the proposed solvent screening methodology for 2-PE/APZ-based absorbents.

3.2. CO₂ absorption performance of 2-PE/APZ-based absorbents

The CO₂ absorption experiments were conducted in three scenarios, (1) simulated flue gas (20v% CO₂), (2) closed space conditions (1v% CO₂), and (3) direct air capture (450 ppm CO₂). A total of 13 2-PE/APZ-based absorbents were used to illustrate the effects of solvents and activators on their CO₂ capture performance in the three scenarios. The results are presented in Fig. 2. To better compare the absorption performance among different absorbents, absorption efficiency calculated by Eq. (1), rather than absorption rate is utilized in following section.

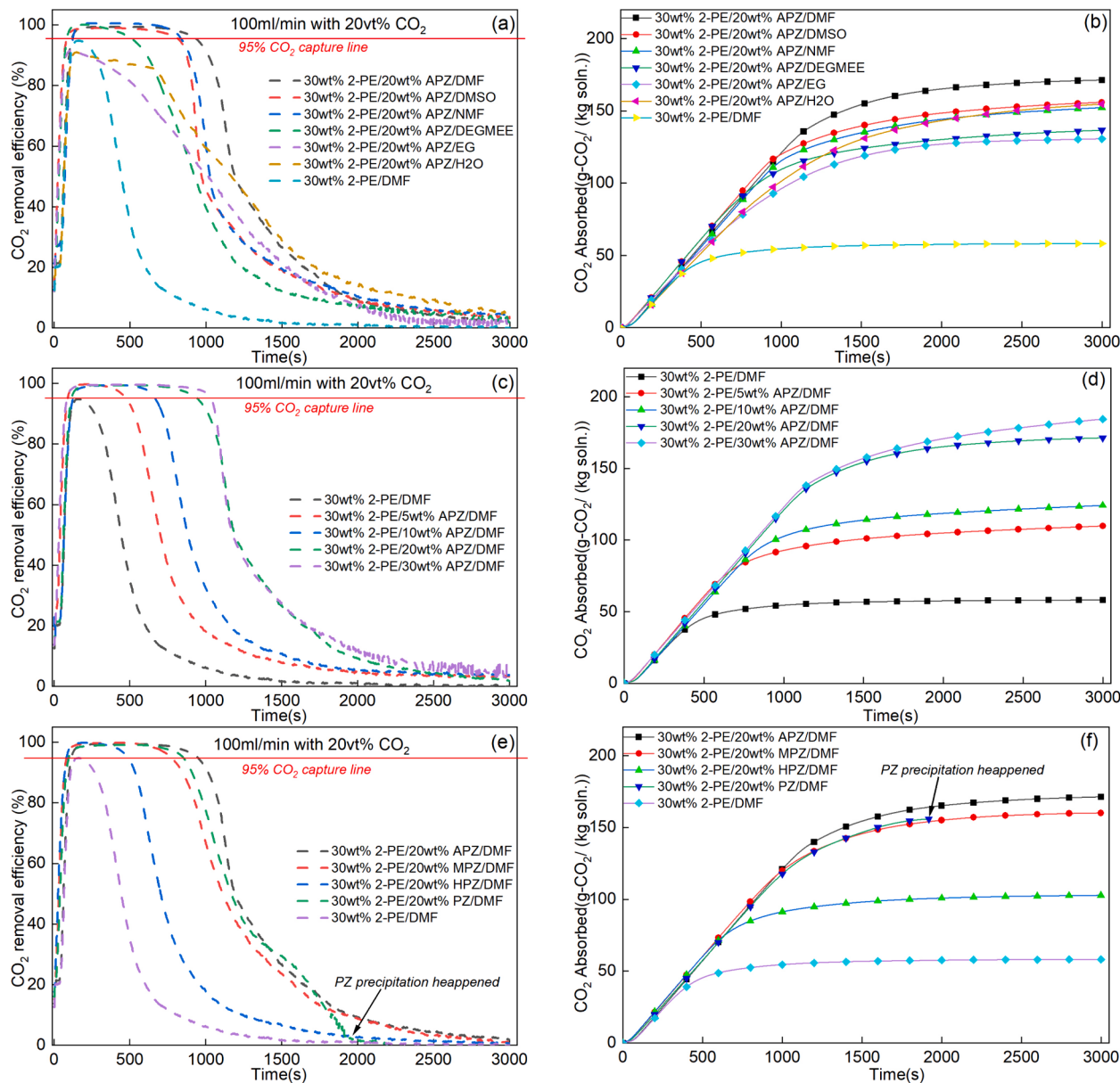


Fig. 2. CO₂ absorption profiles of 2-PE/APZ-based absorbents at 298 K and 1 atm condition. (a) CO₂ removal efficiency of 30 wt% 2-PE 20 wt% APZ with different solvents; (b) CO₂ absorption capacity of 30 wt% 2-PE 20 wt% APZ with different solvents; (c) CO₂ removal efficiency of 30 wt% 2-PE/DMF with different APZ concentration; (d) CO₂ absorption capacity of 30 wt% 2-PE/DMF with different APZ concentration; (e) CO₂ removal efficiency of 30 wt% 2-PE/DMF with 20 wt% APZ, MPZ, HPZ and PZ; (f) CO₂ absorption capacity of 30 wt% 2-PE/DMF with 20 wt% APZ, MPZ, HPZ and PZ;

$$\eta_{abs} = \left(\frac{r_{abs}}{r_{CO_2 input}} \right) * 100 \quad (1)$$

3.2.1. CO₂ capture from simulated flue gas

The MD simulation has predicted that the aprotic solvents coupled with 2-PE/APZ possessed the best absorption performance in section 3.1. To validate the simulation results, the absorption experiments were conducted and presented in Fig. 2. The results indicate that the effect of solvents on CO₂ absorption performance of 2-PE/APZ-based absorbents was ranked as: aprotic solvents (DMF, DMSO, NMF) > ethers (DEGMEE) > alcohols (EG), which agreed well with the MD simulation results.

The 2-PE/DMF binary absorbents showed quite poor absorption performance. Without the addition of APZ, the CO₂ absorption capacity of 2-PE/DMF is much lower than MEA-H₂O. At the same amine concentration (30 wt%), the absorption capacity of 2-PE/DMF is 48.3 % of the MEA-H₂O (120 g-CO₂/(kg-soln.)), which is only 48.3 % of the MEA-H₂O (120 g-CO₂/(kg-soln.)),

). However, the addition of 20 wt% APZ to 2-PE/DMF results in a more than threefold increase in CO₂ absorption efficiency and capacity. With the combination of 2-PE and APZ in aprotic solvents, more than 95 % of the CO₂ was absorbed in approximately 15 mins (15.8, 13.7, and 14.1 min for DMF, DMSO, and NMF as solvents, respectively). This demonstrates the synergistic effect of 2-PE and APZ in enhancing absorption performance. Among the tested absorbents, CO₂ absorption of 2-PE/APZ/DMF achieved the theoretical maximum of 1.004 (mole CO₂/mole amine), with an absorption capacity at 171.31 g-CO₂/(kg-soln.).

DMF, as the most effective solvent for CO₂ absorption in terms of both loading and kinetics, highlights the importance of examining APZ addition ratios in 2-PE/APZ/DMF mixtures. The 2-PE/APZ/DMF absorbents fixed the 2-PE concentration at 30 wt%, and ranged APZ concentrations from 0 wt% to 30 wt%, showing a clear increase in CO₂ capture efficiency with higher APZ levels. As seen from Fig. 2(c) and

(d), increasing APZ from 0 wt% to 5 wt% significantly boosts absorption capacity from 58.17 to 102.77 g-CO₂/(kg-soln.) and speeds up the process (t_{95} from 142 to 476 s). Data shows progressive improvements in capture performance with more APZ; However, excessive addition of the APZ concentration provides limited enhancement to CO₂ uptake; when increasing the APZ concentration from 20 wt% to 30 wt%, the t_{95} times increase from 948 to 1034 s, and the CO₂ absorption capacity increases from 171.31 to 182.61 g-CO₂/(kg-soln.), reflecting only an 8.32 % and 6.19 % increase respectively. The amine efficiency also reduced, with CO₂ loading dropping from 1.004 to 0.892 (mole CO₂/mole amine). This indicates a diminishing return with higher APZ concentrations and emphasizes the optimal mass ratio of 2-PE and APZ could achieve higher absorption performance. Therefore, the best absorption performance is achieved when the concentration of added APZ is 20 wt%.

To systematically investigate the influence of activator type on CO₂ capture performance, we introduced three cyclic amines PZ, HPZ, and MPZ, sharing molecular similarities with APZ, into the 2-PE/DMF absorbent. The results, depicted in Fig. 2(e) and (f), reveal APZ as the top performer in terms of both absorption capacity and rate. The CO₂ absorption capacity of 2-PE/MPZ/DMF is close to that of 2-PE/PZ/DMF, but 2-PE/MPZ/DMF formed precipitation during CO₂ capture, terminating the absorption process and limiting its absorption capacity.

In summary, the superior absorption performance of 2-PE/APZ-based absorbents are attributed to the synergistic effect between 2-PE and APZ, and this synergistic effect was further discussed in Section 3.7. The summarized absorption data is presented in Table 1 for a comprehensive overview.

3.2.2. Carbon capture from super-dilute CO₂ stream (1 v% and 450 ppm)

According to the previous research, the non-aqueous amine absorbents have poor capability to remove CO₂ from gas flows with high flow-rate and super-dilute CO₂ concentration. In this study, the 2-PE/APZ-

Table 1
CO₂ absorption loading, t_{95} , and maximum absorption rate of 2-PE/APZ-based absorbents at 298 K and 1 atm condition with 100 ml/min simulated flue gas.

Absorbents (mass ratio of components)	n _{CO₂} / n _{amine} CO ₂ loading	CO ₂ absorption (g-CO ₂ / kg- soln.)	Maximum r _{abs} rate (g-CO ₂ / (kg-soln. ·min.))	t ₉₅ (s)
2-PE:APZ:DMF (3:2:5)	1.004	171.31	7.78	948
2-PE:APZ:DMSO (3:2:5)	0.941	160.47	7.77	864
2-PE:APZ:NMF (3:2:5)	0.911	155.34	7.77	929
2-PE:APZ:DEGMEE (3:2:5)	0.801	136.52	7.63	524
2-PE:APZ:EG(3:2:5)	0.766	130.66	7.16	0
2-PE:APZ:H ₂ O (3:2:5)	0.907	154.67	7.12	0
2-PE:APZ:DMF (3:2:5)	1.004	171.31	7.78	948
2-PE:PZ:DMF(3:2:5)	0.767	156.91	7.75	773
2-PE:HPZ:DMF (3:2:5)	0.605	102.77	7.65	501
2-PE:MPZ:DMF (3:2:5)	0.842	160.05	7.74	850
2-PE:DMF(3:0:7)	0.566	58.17	7.42	142
2-PE:APZ:DMF (3:0.5:6.5)	0.917	109.80	7.75	476
2-PE:APZ:DMF (3:1:7)	0.931	127.20	7.77	668
2-PE:APZ:DMF (3:2:5)	1.004	171.31	7.78	948
2-PE:APZ:DMF (3:3:4)	0.892	185.61	7.79	1034

t₉₅ (s) presents the absorption time during which the absorption efficiency is higher than 95%.

based absorbents were developed to effectively remove CO₂ from low CO₂ concentration gas sources, such as closed space (1v%) and DAC (450 ppm) scenarios. Fig. 3(a), (b), and (c) correspond to the absorption of 1v% CO₂ by 2-PE/APZ-based absorbents with different solvents, 2-PE/DMF absorbents with different APZ concentrations, and 2-PE/DMF with different cyclic amine activators, respectively. Fig. 3(d) presents the results for DAC by the selected 2-PE/APZ-based absorbents.

As shown in Fig. 3(a), when the gas flow-rate is increased from 100 ml/min to 400 ml/min and CO₂ concentration is reduced to 1 %, the CO₂ absorption performance of 2-PE/APZ-based absorbents with aprotic solvents is much better than that of conventional MEA-H₂O. The maximum absorption efficiency for 2-PE/APZ with aprotic solvents is all above 90 %, while only 81.31 % for MEA-H₂O. The solvents used in the mixture have a significant impact on CO₂ absorption. For example, 2-PE/APZ/DMF (where DMF is solvent) gives a maximum absorption efficiency of 96.50 % and maintains an absorption efficiency above 90 % for over 36 min. When 2-PE/APZ-based absorbents are mixed with water, ethers, and glycols, their absorption efficiency for the same CO₂ stream decreases significantly. 2-PE/APZ/DEGMEE, 2-PE/APZ/EG, and 2-PE/APZ/H₂O show maximum efficiencies of 84.59 %, 56.40 %, and 73.39 %, respectively.

Fig. 3(b) explores the absorption efficiency of 2-PE/DMF with APZ concentrations ranging from 0 wt% to 30 wt%. With APZ concentration increased, the maximum absorption efficiency is 80.76 %, 90.91 %, 93.94 %, 96.50 % and 91.62 % for 0 wt% APZ, 5 % APZ, 10 % APZ, 20 wt % APZ and 30 wt% APZ, respectively. 20 % of APZ gives the highest absorption efficiency. Further increasing APZ from 20 wt% to 30 wt%, the maximum absorption efficiency decreased from 96.50 % to 91.62 %, and the duration of maintaining absorption efficiency above 90 % decreased from 36.3 to 16.2 min.

Fig. 3(c) shows the effect of cyclic amine activators on the CO₂ absorption performance in 30 wt% 2-PE/DMF. The results indicate that among these activators, only APZ reached over 95 % absorption efficiency, and their performance is ranked as APZ>PZ>MPZ>HPZ. Therefore, the cyclic structure of the activator is not the main reason for the excellent absorption performance of 2-PE/APZ-based absorbents. The synergistic effect between 2-PE and APZ resulted in extremely high absorption kinetics and enabled the absorbents to capture CO₂ from a high flow-rate and super-dilute CO₂ stream.

The DAC experiments are conducted over 50 h. As the high flow-rate gas causes significant MEA-H₂O evaporation, MEA-DEGMEE is used to replace aqueous MEA as the experimental reference in the DAC tests. The DAC experiments with 2-PE/APZ-based absorbents mainly focus on the solvent effect in the mixture on their CO₂ capture capability for ultra-dilute CO₂ stream (450 ppm). For the tested solvents, including aprotic solvents (DMF, DMSO), DEGMEE, and EG, the air flow rate is settled as 400 ml/min. As shown in Fig. 3(d), the MEA-DEGMEE and 2-PE/APZ/DEGMEE exhibit similar trends, with the maximum absorption efficiency being 96 % and then immediately declining. The 2-PE/APZ/DMF and 2-PE/APZ/DMSO demonstrate superior performance in DAC tests. On average, within the first 12 h, 96.08 % and 94.74 % CO₂ in the airflow are captured by 2-PE/APZ/DMF and 2-PE/APZ/DMSO, respectively. Over the first 24 h, these two absorbents removed the total of 87.31 % and 82.36 % CO₂ in the air. In contrast, MEA-DEGMEE, 2-PE/APZ/DEGMEE, and 2-PE/APZ/EG only absorb 68.21 %, 70.91 % and 62.30 % CO₂ from the airflow in 24 h. The lower CO₂ absorption from the use of DEGMEE and EG as solvents is due to their high liquid viscosity and low dielectric constant, emphasizing the importance of solvent effects in DAC experiments.

In general, utilizing non-aqueous absorbents to handle high flow-rate and super-dilute CO₂ stream has always been a challenge due to their low CO₂ absorption kinetics. However, 2-PE/APZ-based absorbents with appropriate solvents and 2-PE/APZ ratio exhibits excellent carbon capture performance from both flue gas and air. The excellent absorption performance originates from the synergistic effect of 2-PE and APZ, which are verified by the IR and NMR spectroscopy, as well as DFT

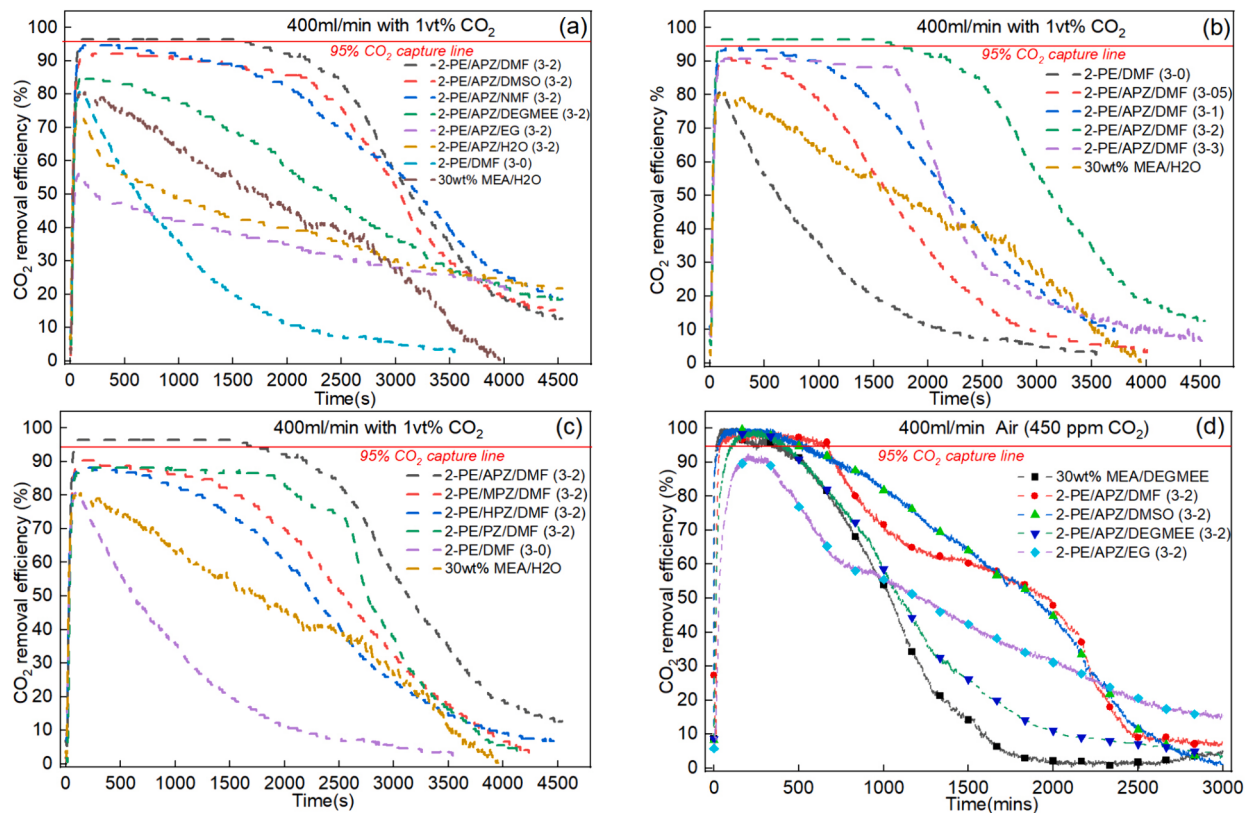


Fig. 3. CO₂ absorption profiles of 2-PE/APZ-based absorbents at 298 K and 1 atm condition. (a) CO₂ removal efficiency of 30 wt% 2-PE 20 wt% APZ with different solvents for flue gas with 1vt% CO₂; (b) CO₂ removal efficiency of 30 wt% 2-PE/DMF with different APZ concentration for flue gas with 1vt% CO₂; (c) CO₂ removal efficiency of 30 wt% 2-PE/DMF with 20 wt% APZ, MPZ, HPZ and PZ concentration for flue gas with 1vt% CO₂; (d) CO₂ removal efficiency of 30 wt% 2-PE 20 wt% APZ with different solvents for CO₂ removal from air (450 ppm CO₂);

calculation in [Section 3.6](#).

3.3. CO₂ desorption performance of 2-PE/APZ-based absorbents

Following the absorption step, the desorption efficiency of 2-PE/APZ-based absorbents is examined at a temperature range from 323 K to 363 K for 40 min. The results are presented in [Figs. 4, 5, and 6](#), where the CO₂ desorption rate is presented in the upper half, and the CO₂ desorbed is shown in the bottom half of each diagram. The effects of various solvents, APZ concentrations, and activators on desorption performance are discussed separately in the following 3 parts. All CO₂ desorption is followed by 20 vt% CO₂ capture experiments.

3.3.1. CO₂ desorption of 2-PE/APZ-based absorbents with various solvents

Similar to CO₂ absorption performance, the solvents used in the 2-PE/APZ-based absorbents have a significant impact on the desorption rate and the desorption efficiency. As shown in [Fig. 4](#), with the desorption temperature increasing from 323 K to 363 K, the maximum desorption rate increased from 12.70 to 39.19 (g-CO₂/ (kg-soln. min.)), from 12.79 to 39.06 (g-CO₂/ (kg-soln. min.)), and from 8.62 to 41.28 (g-CO₂/ (kg-soln. min.)) for 2-PE/APZ/DMF, 2-PE/APZ/DMSO, and 2-PE/APZ/NMF, respectively. Among these solvents, 2-PE/APZ coupled with DMF exhibits the best desorption performance, releasing 157.24 g-CO₂/ (kg-soln.) at 373 K.

$$\eta_{des} = \left(\frac{\alpha_{CO_2rich} - \alpha_{CO_2poor}}{\alpha_{CO_2rich}} \right) * 100 \quad (2)$$

The desorption efficiency is calculated by [eq.2](#) and shown in [Fig. 4\(f\)](#). The use of aprotic solvents (DMF, DMSO, and NMF) provides superior desorption efficiency in comparison to ethers (DEGMEE) and glycols (EG). The desorption efficiencies for 2-PE/APZ/DMF, 2-PE/APZ/DMSO,

and 2-PE/APZ/NMF are 91.41 %, 89.22 %, and 88.15 % at 363 K, respectively. While the desorption efficiency of 2-PE/APZ combined with EG decreased by 7.2 %, with 84.54 % of the CO₂ desorbed at 363 K. Therefore, CO₂ desorption efficiency from 2-PE/APZ/DMF can be achieved over 90 % at 393 K. In contrast, MEA would require at least 413 K to achieve the same desorption efficiency, representing a 25 % increase in temperature.

3.3.2. CO₂ desorption performance of 2-PE/APZ-based absorbent with different concentration

The concentration of the activator affects both absorption and desorption performance. To achieve an optimal balance between absorption performance and desorption efficiency, the APZ to 2-PE ratio needs to be carefully controlled. In our investigation, the activator (APZ) concentration was adjusted at levels of 0 wt%, 5 wt%, 10 wt%, 20 wt% and 30 wt% respectively, while the 2-PE concentration was maintained at 30 wt% in the DMF solvent.

As depicted in [Fig. 5](#), an increase in APZ concentration resulted in a decrease in desorption efficiency but more CO₂ desorbed. This is because, with the addition of APZ, more CO₂ is absorbed, leading to a significant increase in the amount of desorption. For example, at 363 K desorption temperature, in the absence of APZ, the desorption efficiency of 30 wt% 2-PE/DMF can reach 96.72 %, but only 56.69 g-CO₂/ (kg-soln.) is desorbed. As the concentration of added APZ increases to 5 wt %, 10 wt%, 20 wt%, and 30 wt%, although their desorption efficiencies decreased to 93.68 %, 92.48 %, 91.41 %, and 86.56 % at 363 K, due to their significant improved CO₂ absorption capacity, the desorbed CO₂ could reach to 102.86, 115.01, 157.24 and 159.42 g-CO₂/ (kg-soln.), respectively. As seen from [Fig. 5\(f\)](#), when the APZ concentration reached 30 wt%, their desorption efficiency dropped significantly. This could be due to the negative effect of the activator-CO₂ reaction during

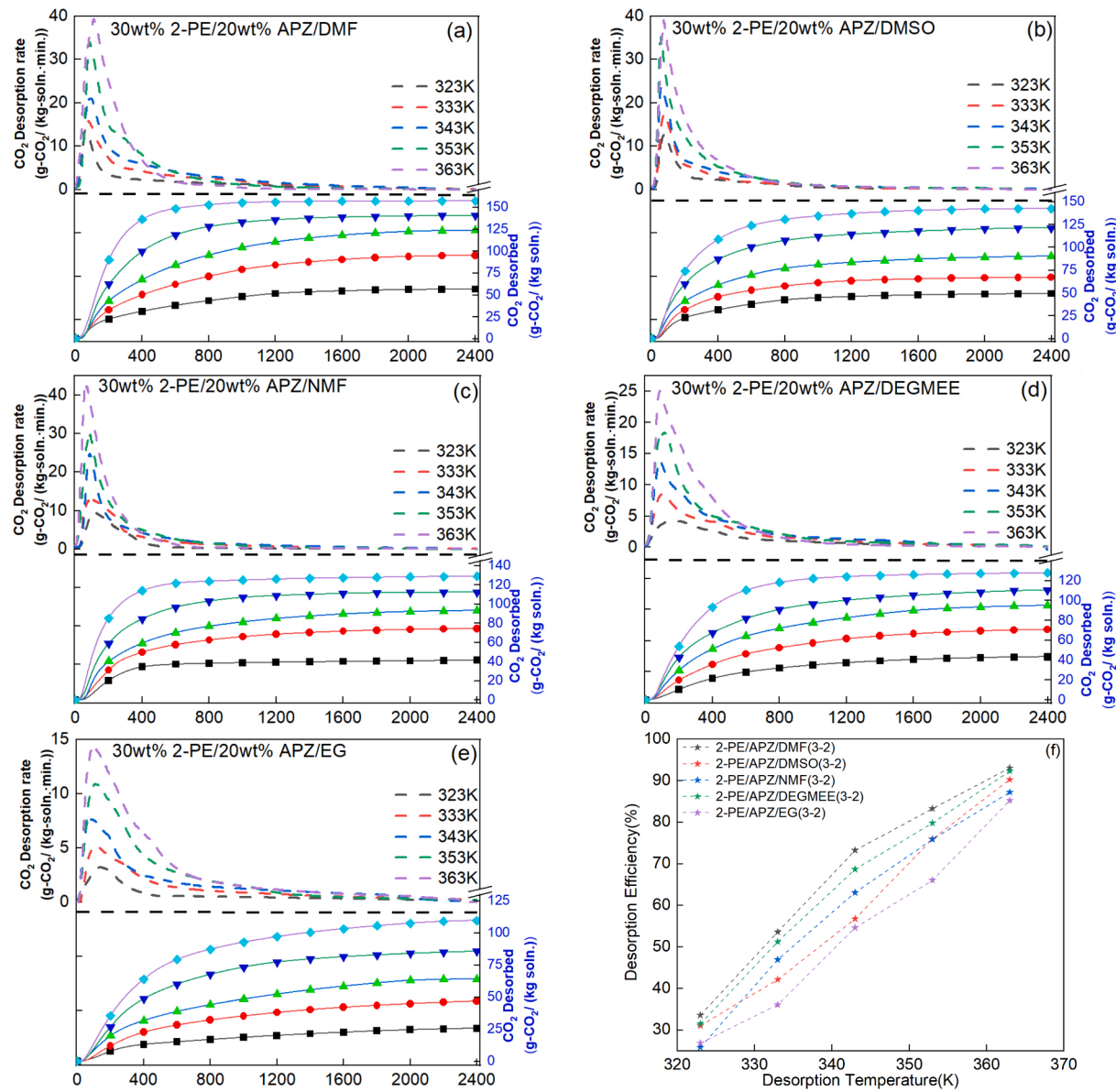


Fig. 4. CO₂ desorption profiles of 2-PE/APZ-based absorbents with various solvents ranged from 323 to 363 K (a) 30 wt% 2-PE 20 wt% APZ DMF; (b) 30 wt% 2-PE 20 wt% APZ DMSO; (c) 30 wt% 2-PE 20 wt% APZ NMF; (d) 30 wt% 2-PE 20 wt% APZ DEGMEE; (e) 30 wt% 2-PE 20 wt% APZ EG; (f) Desorption efficiency of tested absorbents.

CO₂ absorption, and the effect increases with the ratio of APZ in the adsorbents. APZ exhibits a proclivity for proton binding with the activator as opposed to 2-PE; these strong combinations between CO₂ and APZ led to poor desorption performance. This indicates a trade-off point for the addition APZ concentration, an appropriate concentration of APZ in 2-PE/APZ-based absorbent can enhance its absorption ability and maintain the low-temperature regeneration ability. For 2-PE/APZ based absorbents, 20 wt% APZ is the optimal ratio to achieve both good CO₂ absorption and desorption performance coupled with high energy efficiency.

3.3.3. CO₂ desorption of 2-PE/APZ-based absorbent with different activators

As depicted above, the APZ and its concentration in the absorbent play a critical role in both the absorption and desorption performance of 2-PE/APZ-based absorbents. When the mass ratio of 2-PE to APZ is 3:2 (30 wt% 2-PE/20 wt% APZ), the absorbent holds the highest CO₂ absorption loading and maintains more than 90 % desorption efficiency.

To further investigate the effect of activator types on desorption performance, another two cyclic amines (HPZ and MPZ) with similar structures to APZ are mixed with 2-PE/DMF, forming three absorbents, 2-PE/APZ/DMF, 2-PE/MPZ/DMF and 2-PE/HPZ/DMF.

As shown in Fig. 6, among these three absorbents, 2-PE/APZ/DMF exhibited the best desorption capacity, reaching 155.378 (g-CO₂/(kg-soln.)) at 363 K. The 2-PE/MPZ/DMF have the highest desorption kinetics, reaching to 60.32 (g-CO₂/(kg-soln. min.)) at 363 K. Because both MPZ and 2-PE are sterically hindered amines (SHA), the steric hindrance effect may accelerate the desorption rate. The poor desorption performance of 2-PE/HPZ/DMF may be attributed to the hydroxyl group on HPZ, which likely leads to the formation of numerous hydrogen bonds, thereby hindering desorption. In summary, not all cyclic amine is a suitable activator in 2-PE/APZ-based absorbents, hydroxyl groups can significantly weaken the desorption performance.

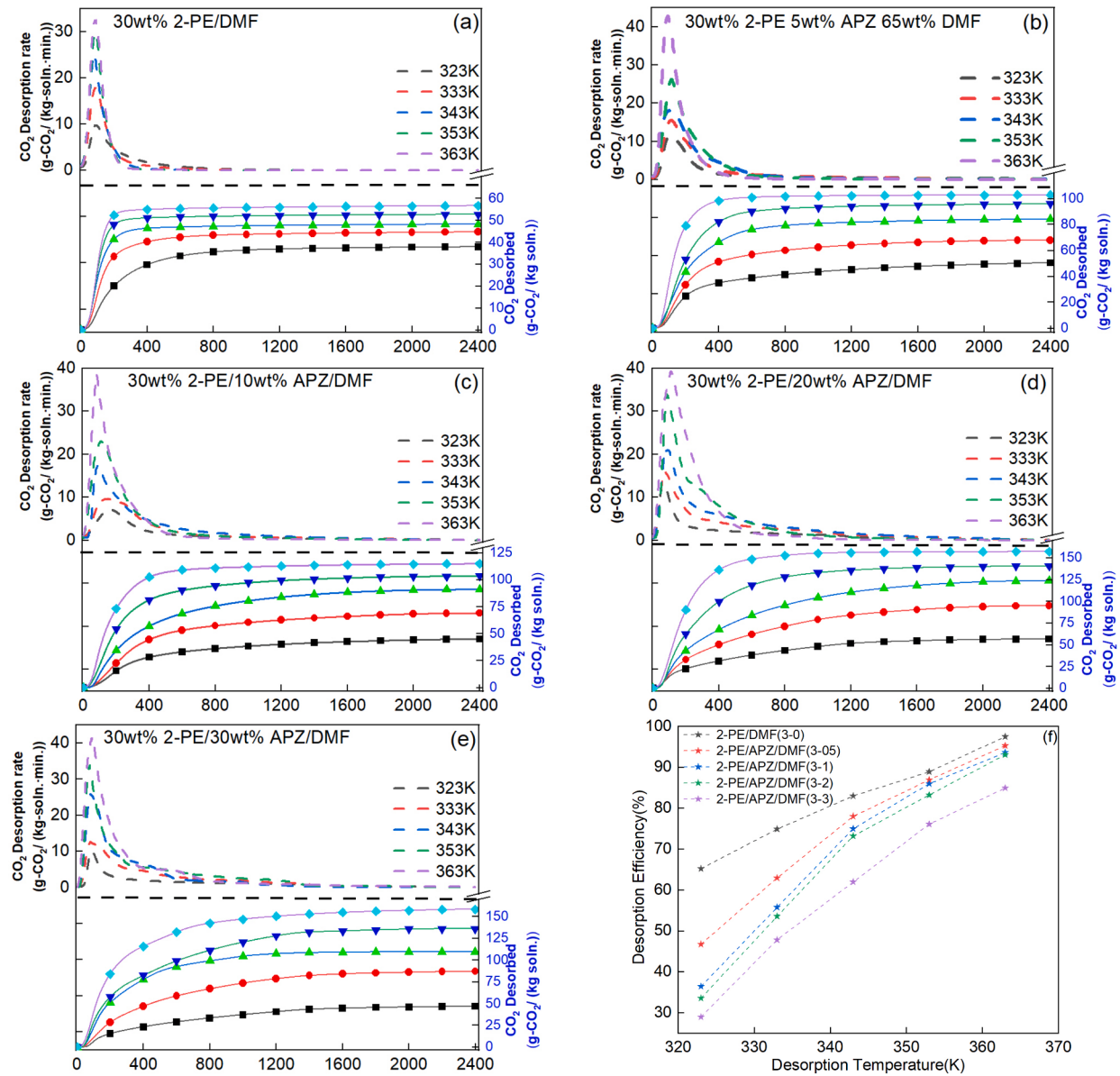


Fig. 5. CO₂ desorption profiles of 2-PE/APZ-based absorbents with various solvents ranged from 323 to 363 K; (a) 30 wt% 2-PE DMF; (b) 30 wt% 2-PE 5 wt% APZ DMF; (c) 30 wt% 2-PE 10 wt% APZ DMF; (d) 30 wt% 2-PE 20 wt% APZ DMF; (e) 30 wt% 2-PE 30 wt% APZ DMF; (f) Desorption efficiency of tested absorbents.

3.4. Comparison of the absorption/desorption performance of 2-PE/APZ-based absorbents with MEA

As the conventional 30 wt% MEA-H₂O is regarded as the benchmark CO₂ capture agents in the industry. For making sure the developed 2-PE/APZ-based have the potential to replace the conventional MEA as the next generation CO₂ capture agents, a series of comparative experiments of MEA and 2-PE/APZ-based absorbents were conducted.

3.4.1. The comparison of the 2-PE/APZ-based absorbents with 30 wt% MEA-H₂O

As discussed in [Section 3.2](#), 2-PE/APZ-based absorbents have demonstrated the excellent CO₂ capture performance. As shown in [Fig. 7\(a\)](#), in comparison to the 30 wt% MEA-H₂O, the 2-PE/APZ/DMF (3-2) demonstrated a maximum CO₂ absorption rate of 7.78 g·CO₂/ (kg·soln·min.) for 15 min, while the MEA has an initial absorption rate of 7.12 g·CO₂/ (kg·soln·min.) and dropped immediately within 3 mins. The CO₂ absorption behaviour in 2-PE/APZ based absorbents is distinctly different from that in MEA. As beginning of absorption, nearly all the

CO₂ is captured by 2-PE/APZ/DMF, which the absorption curves are overlapped, after 15 min, the absorption curve just starting declining. In contrast, the MEA absorption rate reached to the top at the beginning CO₂ capture then spreading out quickly. This indicates that the absorption performance of 2-PE/APZ-based absorbents is limited by the supplied amount of CO₂ and that the absorption kinetics was greatly improved in comparison to the MEA. The [Fig. 7\(b\)](#) demonstrated the CO₂ desorption of 2-PE/APZ based absorbents with 30 wt% MEA-H₂O. The desorption kinetics of 2-PE/APZ/DMF (3-2) is approximately 1.5 times that of 30 wt% MEA-H₂O (39.4 vs 27.1 g·CO₂/ (kg·soln·min.)). Even for single amine 2-PE/DMF absorbents, the desorption rate is still higher than that of MEA (32.6 vs 27.1 g·CO₂/ (kg·soln·min.)). It indicated that the optimum desorption temperature of 2-PE/APZ-based absorbents is 393 K, much lower than that of MEA (393–413 K). This also suggests that in anhydrous condition, the 2-PE/APZ-CO₂ products are much easier to decompose than MEA-CO₂ in aqueous condition.

[Fig. 8](#) summarizes the absorption capacity, CO₂ desorbed amount, and regeneration efficiency of 2-PE/DMF (3-0), 2-PE/APZ/DMF (3-2), 2-PE/APZ/DMSO (3-2) and 30 wt% MEA-H₂O. These results indicate

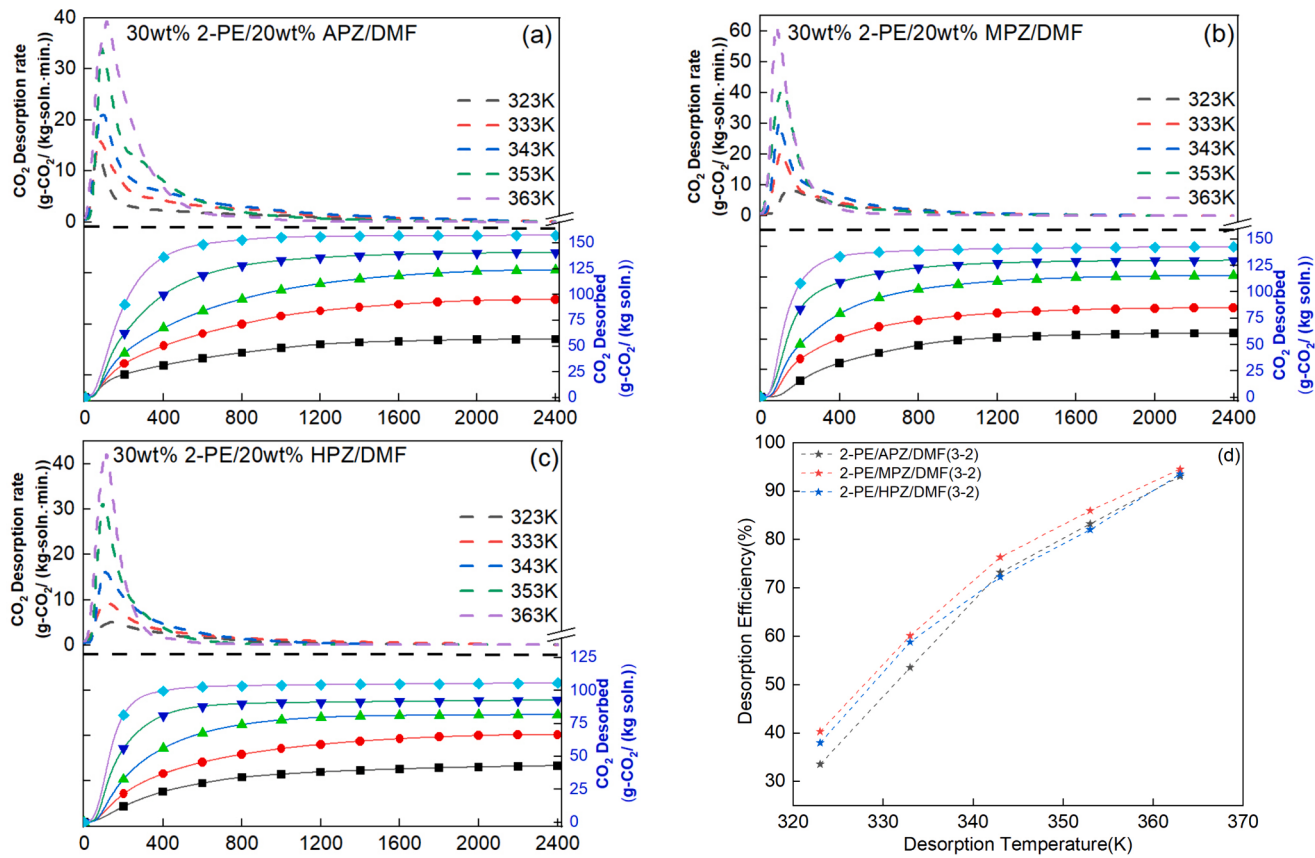


Fig. 6. CO₂ desorption profiles of 2-PE/APZ-based absorbents with various solvents ranged from 323 to 363 K; (a) 30 wt% 2-PE/DMF; (b) 30 wt% 2-PE 5 wt% APZ DMF; (c) 30 wt% 2-PE 10 wt% APZ DMF; (d) Desorption efficiency of tested absorbents.

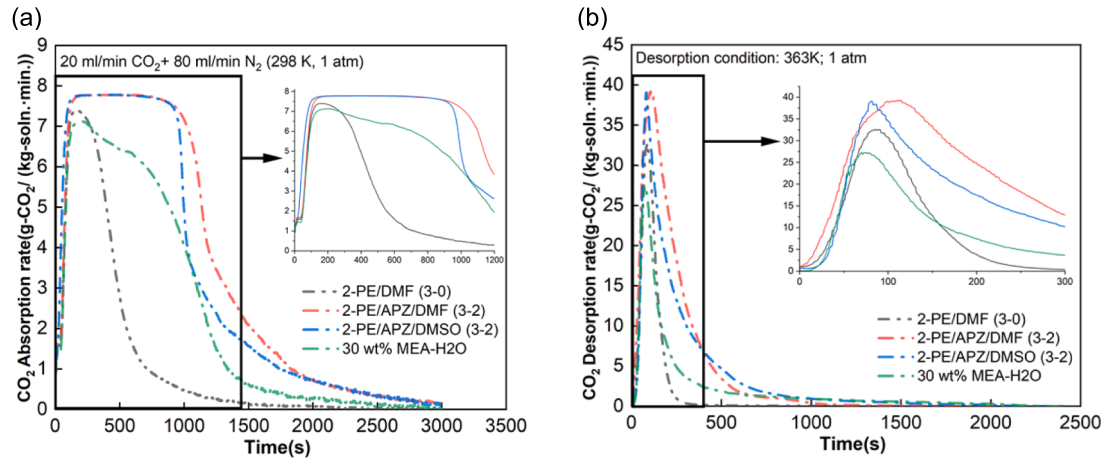


Fig. 7. The comparison of CO₂ absorption/desorption kinetics of 2-PE/DMF (3-0), 2-PE/APZ/DMF (3-2), 2-PE/APZ/DMSO (3-2), and with 30 wt% MEA-H₂O; (a): Absorption kinetics at 298 K, 1 atm with 20 ml/min CO₂ and 80 ml/min N₂; (b) Desorption kinetics at 363 K, 1 atm with 100 ml/min N₂.

that, at the same desorption temperature (363 K), the 2-PE/APZ based absorbents always exhibit higher regeneration efficiency than 30 wt% MEA-H₂O. Moreover, the addition of APZ into 2-PE/DMF system further improve the absorption capacity and CO₂ desorbed amount significantly. MEA-H₂O, as a commonly used industrial CO₂ absorbents, has an absorption capacity of 120 g·CO₂/ (kg·soln.), and its regeneration efficiency was only 70.3 % at 363 K. In contrast, the CO₂ absorption capacity of 2-PE/APZ/DMF (3-2) is 171 g·CO₂/ (kg·soln.), which is 30 % higher than that of MEA-H₂O, and its regeneration efficiency reaches to 91.8 % at 363 K, which means 157 g·CO₂/ (kg·soln.) is desorbed, 45.8 %

higher than that of MEA. High desorption efficiency means that the cyclic adsorption capacity of 2-PE/APZ based absorbents is much higher than the benchmark absorbent MEA-H₂O, indicating the great potential to be applied in industry as energy-saving absorbent for CO₂ capture.

3.4.2. The comparison of the 2-PE/APZ-based absorbents with aqueous/non-aqueous MEA absorbents

To further understand the superior performance of our developed 2-PE/APZ-based absorbents, we considered the contribution from the amount of amine molecular in the absorbents. To eliminate the influence

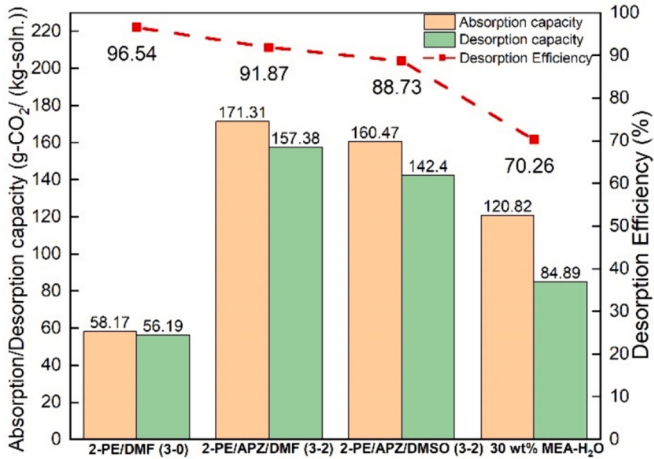


Fig. 8. The comparison of CO₂ absorption/desorption capacity and regeneration efficiency of 2-PE/DMF (3-0), 2-PE/APZ/DMF (3-2), 2-PE/APZ/DMSO (3-2), and with 30 wt% MEA-H₂O; absorption at 298 K and desorption at 363 K.

from the available amine molecular in the absorbents, we adjust the portion of amine in the MEA absorbents to the same level as 2-PE/APZ-based absorbents, then conducting the comparative experiments. The developed 2-PE/APZ-based absorbents and conventional MEA differ in molar concentration, for example, the molar concentration of 2-PE/APZ/DMF (3-2) is 3.87 mol/L, whereas 30 wt% MEA is 5 mol/L. Therefore, we used 50 wt% MEA and 3.87 mol/L (23.5 wt%) MEA absorbents as the reference absorbent, as they share the same mass and molar concentrations with the 2-PE/APZ (3-2) absorbents. The absorption kinetics of MEA and 2-PE/APZ-based absorbents are shown in Fig. 9. Two of the best-performing 2-PE/APZ-based absorbents, 2-PE/APZ/DMF (3-2) and 2-PE/APZ/DMSO (3-2), were selected. MEA-based absorbents included MEA-H₂O, MEA-DEGMEE, and MEA-EG. When MEA was mixed with DMF, DMSO, or NMF, precipitation formed during CO₂ absorption/desorption. As illustrated in Fig. 9(a), under 100 ml/min simulated flue gas flow (20 v% CO₂), 2-PE/APZ/DMF (3-2) and 2-PE/APZ/DMSO (3-2) exhibited absorption rates of 7.78 and 7.77 g-CO₂/(kg-soln·min.) respectively, maintaining this rate for more than 15 min. In contrast, the maximum CO₂ absorption rate of aqueous MEA was 6.81 g-CO₂/(kg-soln·min.) (23.5 wt% MEA-H₂O) and 7.15 g-CO₂/(kg-soln·min.) (50 wt% MEA-H₂O). Even the non-aqueous MEA such as 50 wt% MEA-DEGMEE, possessing a lower maximum absorption

rate (7.55 g-CO₂/(kg-soln·min.)) than 2-PE/APZ-based absorbents. In the 100 ml/min flue gas absorption experiments, the CO₂ absorption rate of 2-PE/APZ-based absorbents were limited by the supplied CO₂ amount, prompting the input flue gas flow rate could further explore the absorption performance. When the flue gas rate was increased to 200 ml/min (Fig. 9(b)), the 2-PE/APZ-based absorbents still have excellent absorption rates. At beginning of absorption, the 2-PE/APZ/DMF (3-2) and 2-PE/APZ/DMSO (3-2) reached to the maximum absorption rates, which were 15.52 and 15.53 g-CO₂/(kg-soln·min.), absorbing almost all CO₂ for approximately 10 min. In contrast, the MEA absorption rate reached to the top at the beginning CO₂ capture then declining quickly. Among the tested MEA, the highest absorption rate is achieved by 50 wt% MEA-DEGMEE (15.27 g-CO₂/(kg-soln·min.)), but it precipitated around 14 min as shown in Fig. 9(b), whereas 2-PE/APZ-based absorbents remained clear and homogeneous throughout the process.

These results indicate that the absorption kinetics of 2-PE/APZ-based absorbents are significantly better than those of MEA at the same mass or molar concentrations. Moreover, the CO₂ loading of 2-PE/APZ/DMF is 1.004 (one mole amine can absorb one mole CO₂). For MEA absorbents, the absorption loading was only around 0.5, and higher concentration MEA had lower absorption loading (50 wt% MEA-H₂O=0.467, 50 wt% MEA-EG=0.508, and 50 wt% MEA-DEGMEE=0.431). It indicated that the amine in the 2-PE/APZ-based absorbents are utilized more efficient. This high amine utilization of 2-PE/APZ-based absorbents can improve molecular economy and lead to more sustainable carbon capture. The Absorption data are summarized at Table 2.

3.4.3. The desorption comparison of the 2-PE/APZ-based absorbents at 363 K with MEA absorbents at 393 and 341 K

The previous section, we compare the desorption performance of our developed solvents with the benchmark 30 % MEA at the same temperature of 363 K. To further understand the supervisor desorption performance of our developed 2-PE/APZ-based absorbents, the comparison was conducted at their optimum temperature of the solvents. For CO₂ desorption, the 2-PE/APZ based absorbents demonstrated more than 90 % desorption efficiency at 363 K, while the optimum regeneration temperature for MEA-CO₂ was ranged from 393 to 413 K. In order to further compare the desorption performance of 2-PE/APZ and MEA at their optimum regeneration temperature, the CO₂ saturated MEA were heated to 393 and 413 K, then comparing their desorption kinetics with 2-PE/APZ/DMF and 2-PE/APZ/DMSO at 363 K. The results are summarized at Fig. 10.

As shown in Fig. 10(a), under the 393 K desorption temperature, 50 wt% MEA-DEGMEE gave the best desorption performance among the tested MEA absorbents, but was still not as effective as the 2-PE/APZ

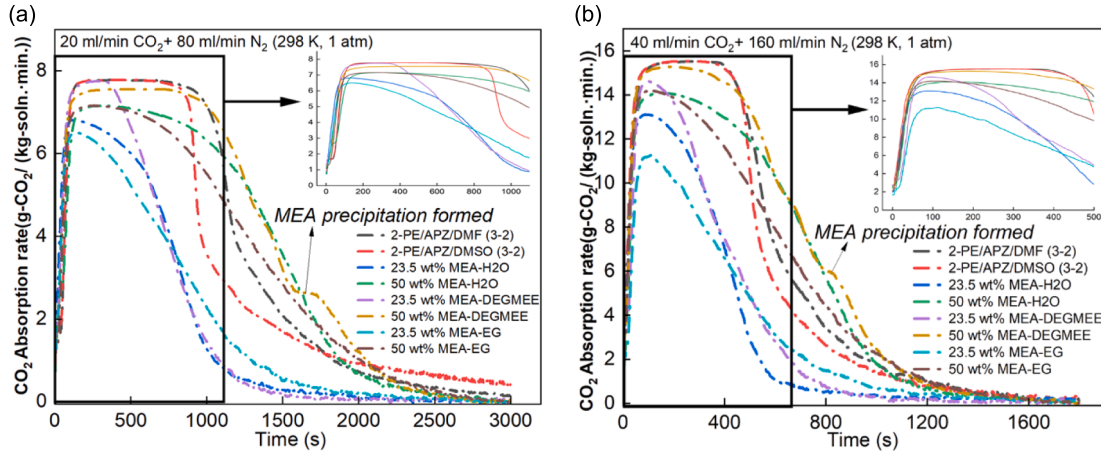


Fig. 9. The comparison of CO₂ absorption kinetics of 2-PE/APZ/DMF (3-2), 2-PE/APZ/DMSO (3-2), 23.5 wt% MEA-H₂O, 50 wt% MEA-H₂O, 23.5 wt% MEA-DEGMEE, 50 wt% MEA-DEGMEE, 23.5 wt% MEA-EG, and 50 wt% MEA-EG. (a) Absorption condition: 20 ml/min CO₂, 80 ml/min N₂ under 298 K and 1 atm; (b) Absorption condition: 40 ml/min CO₂, 160 ml/min N₂ under 298 K and 1 atm.

Table 2

Absorption data of aqueous/non-aqueous MEA and 2-PE/APZ-based absorbents under 298 K and 1 atm.

	Flue gas flow rate ml/min (20 wt% CO₂)	Maximum <i>r</i>_{abs} (g-CO₂/(kg-soln. ·min.))	Absorption capacity (g-CO₂ / kg-soln.)	Absorption loading (mole CO₂/mole amine)
MEA-H ₂ O (23.5 wt %)	100 ml/min	6.81	91.75	0.538
	200 ml/min	13.10	90.68	0.532
MEA-H ₂ O (50 wt%)	100 ml/min	7.15	171.51	0.464
	200 ml/min	14.09	170.37	0.467
MEA-DEGMEE (23.5 wt %)	100 ml/min	7.72	96.92	0.569
	200 ml/min	14.62	100.92	0.582
MEA-DEGMEE (50 wt%)	100 ml/min	7.55	187.88	0.508
	200 ml/min	15.27	187.77	0.514
MEA-EG (23.5 wt %)	100 ml/min	6.51	93.65	0.549
	200 ml/min	11.27	89.96	0.528
MEA-EG (50 wt%)	100 ml/min	7.16	162.73	0.440
	200 ml/min	14.18	157.14	0.431
2-PE/APZ/ DMF (3-2)	100 ml/min	7.78	171.31	1.004
	200 ml/min	15.52	171.78	0.997
2-PE/APZ/ DMSO (3-2)	100 ml/min	7.77	160.47	0.941
	200 ml/min	15.53	159.31	0.935

based absorbents. Although the maximum desorption rates of 50 wt% MEA-DEGMEE and 2-PE/APZ/DMF were almost the same (39.68 g-CO₂/(kg-soln.·min.)) vs 39.38 (g-CO₂/(kg-soln.·min.)), the CO₂ desorption capacity and efficiency of MEA were only 145.93 (g-CO₂ / kg-soln.) and 79.04 %, while 2-PE/APZ/DMF reached 157.995 (g-CO₂ / kg-soln.) and 91.62 %. More importantly, the desorption temperature of 2-PE/APZ/DMF is only 363 K. As shown in Fig. 10(b), when we increase the desorption temperature to 413 K, the desorption efficiency of MEA reaches more than 90 %, especially the 50 wt% MEA-EG, which is 95.62 %. Therefore, MEA can be effectively regenerated at 413 K, which is also the decomposition temperature of MEA-CO₂ products. In comparison,

the decomposition temperature of 2-PE/APZ-CO₂ products is only 363 K, which is 32 % reduction. The comparative experiments results showed that the effective desorption temperature of developed 2-PE/APZ based absorbents decreased from 413 K to 363 K compared to conventional MEA. The 2-PE/APZ based absorbents can serve as a promising alternative for low-energy CO₂ capture. The desorption data is summarized at Table 3 below.

3.5. Thermal stability and regeneration ability of 2-PE/APZ-based absorbents

The previous sections have demonstrated that 2-PE/APZ-based absorbents, mixing with aprotic solvents (DMF, DMSO, NMF), outperform traditional MEA absorbents in CO₂ capture. Experiments designed in this section is to assess their recyclability and thermal stability [42], such as the durability of 2-PE absorbents in cyclic CO₂ capture and their structure stability at 393 K desorption temperatures. 2-PE/DMF, 2-PE/APZ/DMF, 2-PE/APZ/DMSO, and 2-PE/APZ/NMF are used to assess their performance over multiple cycles.

3.5.1. The dynamics cyclic experiments of 2-PE/APZ-based absorbents

Section 3.3 reveals that 2-PE/APZ based absorbents maintain over 90 % desorption efficiency at 393 K regeneration temperature. Five

Table 3

Desorption values of MEA under 393 and 413 K; 2-PE/APZ-based absorbents under 363 K.

	Desorption Temperature (K)	Maximum <i>r</i>_{des} (g-CO₂/(kg-soln. ·min.))	CO₂ desorption (g-CO₂ / kg-soln.)	Regeneration Efficiency (%)
MEA-DEGMEE (23.5 wt %)	393	30.747	83.289	83.29 %
	413	39.176	92.132	92.13 %
MEA-DEGMEE (50 wt%)	393	39.682	145.931	79.04 %
	413	56.965	171.028	90.97 %
MEA-EG (23.5 wt %)	393	22.167	82.536	85.09 %
	413	41.292	90.764	93.57 %
MEA-EG (50 wt%)	393	31.293	143.501	88.03 %
	413	52.153	155.865	95.62 %
2-PE/APZ/ DMF (3-2)	363	39.388	157.995	91.62 %
2-PE/APZ/ DMSO (3-2)	363	39.056	142.403	89.22 %

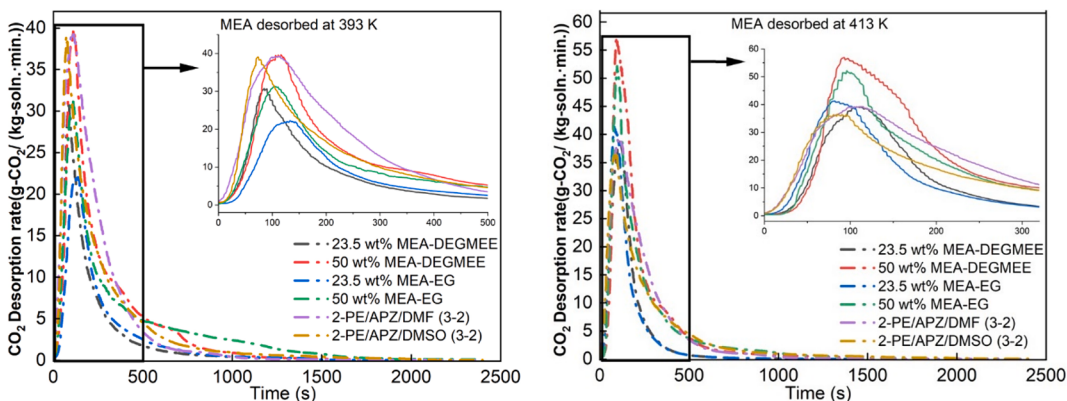


Fig. 10. The comparison of CO₂ desorption kinetics of 2-PE/APZ/DMF (3-2), 2-PE/APZ/DMSO (3-2), 23.5 wt% MEA-DEGMEE, 50 wt% MEA-DEGMEE, 23.5 wt% MEA-EG, and 50 wt% MEA-EG with 100 ml N₂/min purging. (a) Desorption of MEA at 393 K and desorption of 2-PE/APZ based absorbents at 363 K; (b) Desorption of MEA at 413 K and desorption of 2-PE/APZ based absorbents at 363 K;

cycles of absorption at 298 K and desorption at 363 K with N₂ purging were conducted for each absorbent to investigate their recyclability and thermal stability. As depicted in Fig. 11(a) to (d), without APZ, the recycled capacity of 2-PE/DMF is 55.96 (g-CO₂/ kg-soln.) after the 5 cycles. Upon the addition of APZ, the recycled CO₂ capacity of 2-PE/APZ/DMF, 2-PE/APZ/DMSO and 2-PE/APZ/NMF significantly increases from 55.36 to 155.5, 147.6, and 129.7 g-CO₂/(kg-soln.),

respectively. In contrast, for 30 wt% MEA-H₂O, the CO₂ absorption capacity is about 123 (g-CO₂/ (kg-soln.)) in first cycle, but reduce to only 85 (g-CO₂/ kg-soln.) in 5th cycle, which is only 61 % of the initial absorption capacity, where 0.25–0.30 mol CO₂/mol MEA remained in the MEA absorbents after desorption. This result indicates that 2-PE/APZ-based absorbents are more efficient and sustainable for CO₂ capture in industrial applications. For the information, other 2-PE/APZ-based

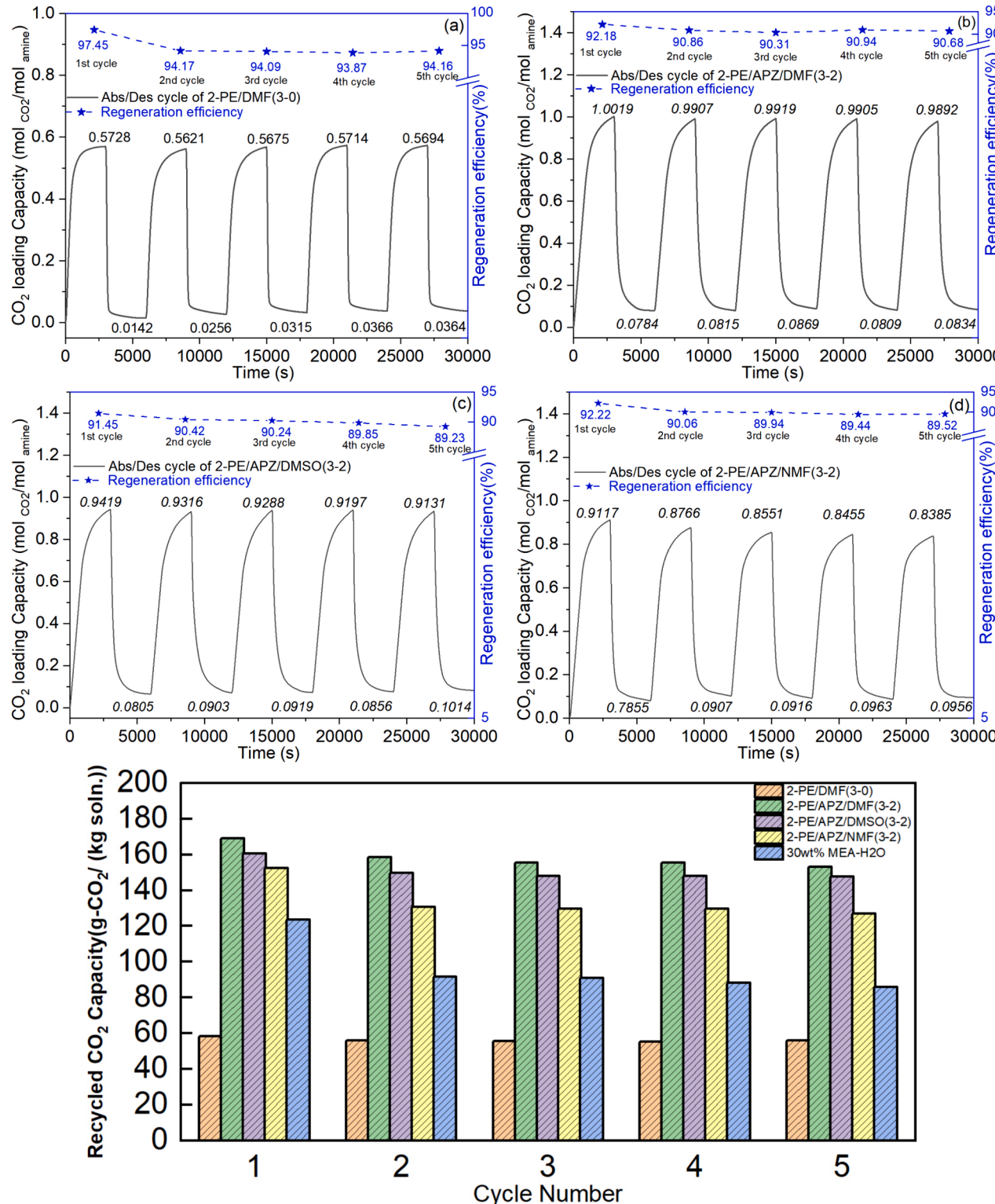


Fig. 11. Dynamics cyclic absorption/desorption performance of 2-PE/APZ based absorbents; a) 2-PE/DMF; b) 2-PE/APZ/DMF; c) 2-PE/APZ/DMSO; d) 2-PE/APZ/NMF; e) The cyclic capacity of 2-PE/APZ-based absorbents compared with 30 wt% MEA. (Desorption condition: 363 K, 100 ml/min N₂ purging flow).

absorbents' dynamics cyclic results are presented in [Supporting Information Part 5](#).

3.5.2. The thermal stability of 2-PE/APZ-based absorbents

The use of absorbents in commercial applications relies on their thermal stability. Typically, the thermal regeneration of amine absorbents causes their chemical degradation. Despite 2-PE/APZ-based absorbents operating at a lower desorption temperature (around 363 K) than MEA (393–413 K), assessing their thermal stability is still crucial [\[43\]](#). NMR spectroscopy is used to examine the molecular stability of 2-PE-based absorbents after 1, 3, and 5 absorption-desorption cycles, at 298 K for CO₂ absorption and 363 K for CO₂ desorption [\[44\]](#). The ¹³C and ¹H NMR, delineated in [Fig. 12](#) and [Fig. S8](#), offer insights into the molecular structure at various cycles. The NMR spectra showed no new peaks or significant peak shifts, indicating that the chemical structure remains unchanged and highlighting the thermal stability of 2-PE/APZ-based absorbents during cycled experiments.

3.6. The desorption energy consumption of 2-PE/APZ-based absorbents

The high energy penalty has been recognized as a significant challenge in CO₂ capture processes. However, the 2-PE-based absorbents developed in this study offer the potential for complete regeneration under mild conditions (363 K). Calculations based on the Arrhenius equation (shown in [Table S2](#)) show that the desorption activation energy of 2-PE/DMF and 2-PE/APZ/DMF (3–2) is 26.823 and 34.613 kJ/mole, indicating a low energy regeneration provided by our developed absorbents, in comparison with benchmark absorbent MEA. To further confirm their low energy consumption, both direct measurement and

theoretical calculations were conducted. Direct measurement is performed using a microwave swing process detailed in [Supporting Information Part 1](#), while theoretical calculation is based on thermodynamic functions including reaction heat, sensible heat, and latent heat, determined through DSC characterization [\[42\]](#).

3.6.1. Energy consumption measured from the microwave swing process

A microwave swing system for CO₂ regeneration was employed to calculate energy consumption during desorption process by measuring the microwave energy difference before and after solvent treatment. A key metric, the energy-to-released CO₂ ratio (EC, in kJ/mol), was used to evaluate regeneration energy consumption efficiency as [eq. 2](#). The results are presented in [Table 4](#), and indicate that the solvents used in the developed absorbents have significant impact on EC values. Notably, DEGMEC showcased the lowest EC (1295 kJ/mole) due to its low dielectric constant (12.6). 2-PE/APZ/DMF (3–2) offers a 54.7 % reduction in EC compared to traditional 30 % MEA solutions.

$$EC_t = \frac{\text{Energy}_t (\text{kJ})}{\text{CO}_2\text{stripped}_t (\text{mol})} \quad (2)$$

The microwave energies measured in this experiment are specific to our setup and not directly comparable to existing literature due to the non-ideal microwave swing process. The measured energy consumption is affected by small samples used (5 g), the partial reactor heated by the microwave, and energy losses due to N₂ purging and heating the quartz reactor. It does not provide absolute values. However, the data can be used for the comparison of the energy consumption for different solvents, as the effect of these factors on the energy consumption is controlled for all of the measurements. To further verify the comparison

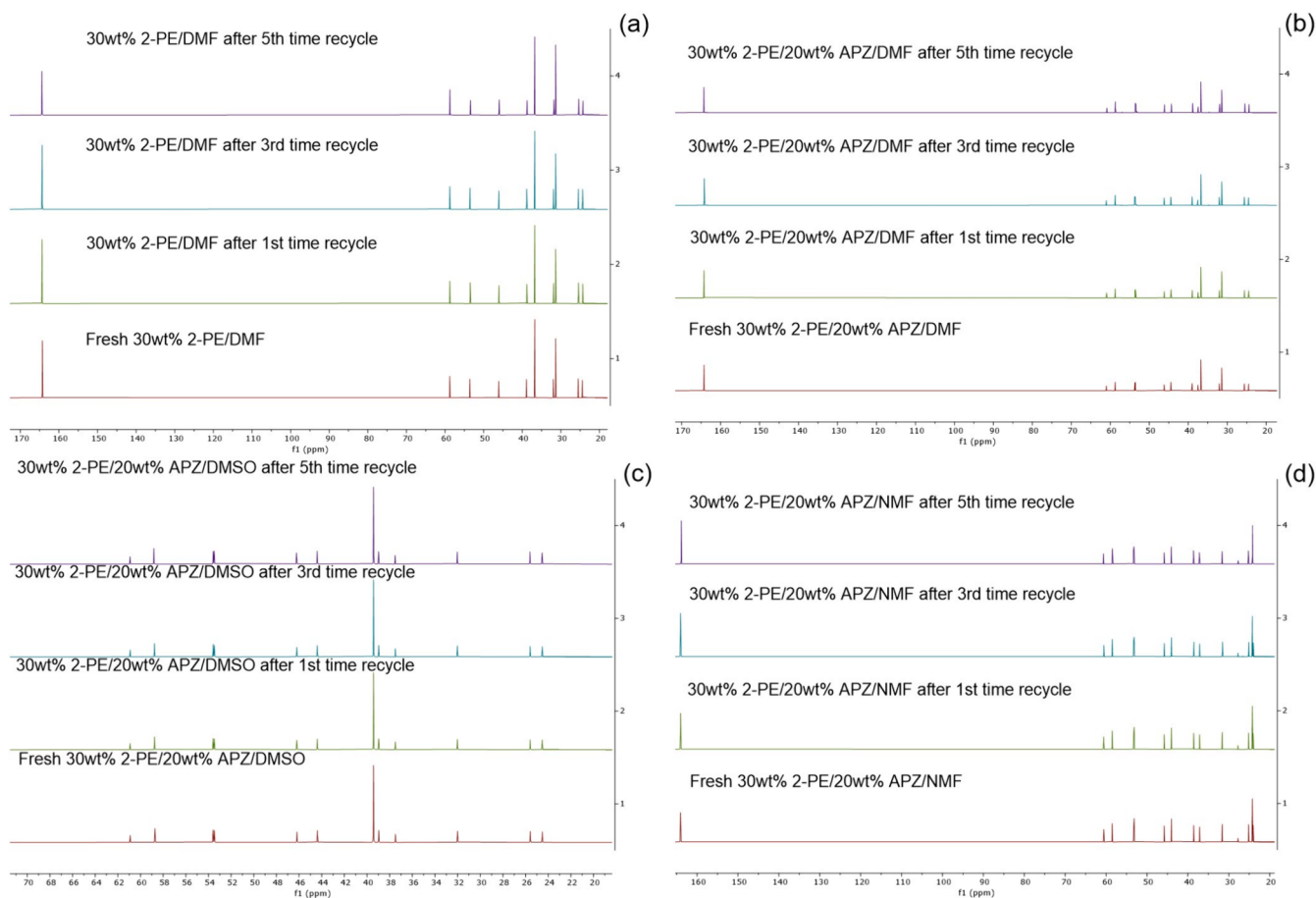


Fig. 12. ¹³C NMR spectrum of recycled 2-PE/APZ-based absorbents; a) 2-PE/DMF (3–0); b) 2-PE/APZ/DMF (3–2); c) 2-PE/APZ/DMSO (3–2); d) 2-PE/APZ/NMF (3–2).

Table 4

The comparison of energy consumption of 2-PE/APZ based absorbents and MEA absorbent at 363 K.

Absorbents	2-PE/ DMF (3-0)	2-PE/ APZ/ DMSO (3-2)	2-PE/ APZ/ NMF (3-2)	2-PE/ APZ/EG (3-2)	2-PE/APZ/ DEGMEE (3-2)
Desorbed amount (mol)	0.00614	0.01618	0.01466	0.01259	0.01451
Energy (kJ)	14.0914	27.9100	29.6640	29.9850	18.7990
t_{95} time(s)	241	927	640	1295	1017
EC _r (kJ/mol)	2296.51	1724.97	2023.46	2381.65	1295.58
	2-PE/ APZ/ DMF (3-0)	2-PE/ APZ/ DMF (3-1)	2-PE/ APZ/ DMF (3-2)	2-PE/ APZ/ DMF (3-3)	Aqueous 30 wt% MEA [16]
Desorbed amount (mol)	0.01124	0.01364	0.01787	0.01736	0.00440
Energy (kJ)	19.3068	22.4198	24.7760	34.6380	16.1290
t_{95} time(s)	479	605	644	1231	—
EC _r (kJ/mol)	1717.69	1643.68	1386.46	1995.27	3665.68

of the energy consumption, we also propose an energy consumption calculation based on thermodynamic functions for a more ideal regeneration process.

3.6.2. Energy consumption calculated by thermodynamics functions

The energy consumption (Q) in CO_2 desorption process consists of three main parts: the sensible heat (Q_s), the reaction heat of desorption (Q_r), and the latent heat of vaporization (Q_v).

For calculating Q_s , the specific heat capacity (C_p) is required. The average C_p for mixtures was calculated based on the molar ratios of components [44], and results are showed in Table 5. The sensible heat of 2-PE/APZ-based absorbents varied from 0.84 to 1.5 KJ/g CO_2 due to their different C_p . Aprotic solvents like DMF, NMF, and DMSO have lower C_p , favouring regeneration.

The reaction heat (Q_r) was determined by TG/DSC analyser, and the DSC plots are presented in Fig. S6. 30 wt% aqueous MEA was used as reference data to verify our measured results. Our measured MEA reaction heat was 1.892 KJ/g CO_2 , which agreed well with the data provided in the literature (1.818–2.5 KJ/g CO_2) [45]. As indicated in Table 5, the reaction heats for 2-PE/APZ-based absorbents with various solvents are comparable (0.73 to 0.86 KJ/g CO_2). As the desorption

Table 5

Regeneration energy of 2-PE/APZ based absorbents estimated by thermodynamics equations.

Absorbents	2-PE/ DMF (3-0)	2-PE/ APZ/ DMSO (3-2)	2-PE/ APZ/ NMF (3-2)	2-PE/ APZ/EG (3-2)	2-PE/APZ/ DEGMEE (3-2)
$C_p(J/(mole^*K))$	166.751	194.861	168.682	186.580	276.075
$Q_{\text{sensibleheat}}$	2.389	0.914	1.048	1.306	1.449
$Q_{\text{reactionheat}}$	1.115	0.813	0.810	0.727	0.804
$Q_{\text{vaporizationheat}}$	0	0	0	0	0
$Q_{\text{total}}(\text{kJ/g CO}_2)$	3.504	1.727	1.858	2.033	2.253
	2-PE/ APZ/ DMF (3-0)	2-PE/ APZ/ DMSO (3-2)	2-PE/ APZ/ NMF (3-2)	2-PE/ APZ/EG (3-2)	Aqueous 30 wt% MEA* [42]
$C_p(kJ/(kg^*K))$	171.791	177.095	188.583	301.417	—
$Q_{\text{sensibleheat}}$	1.224	1.121	0.835	0.867	1.961
$Q_{\text{reactionheat}}$	0.977	0.889	0.859	1.126	1.795
$Q_{\text{vaporizationheat}}$	0	0	0	0	0.068
$Q_{\text{total}}(\text{kJ/g CO}_2)$	2.201	2.010	1.694	1.993	3.84

* The results from literature which calculate in the same method.

temperature (363 K) is significantly lower than the boiling temperatures of components in 2-PE absorbents, latent heat due to solvent vaporization (Q_v) during desorption is negligible.

In conclusion, the regeneration energy calculated agrees well with the values measured by microwave regeneration. The 2-PE/APZ/DMF (3-2) exhibits the energy consumption (Q) of 1.694 KJ/g CO_2 , which was about 55.89 % lower than that of MEA-H₂O and 51.66 % lower than that of single 2-PE/DMF. The synergistic effect of 2-PE and APZ promotes significant energy reduction.

3.6.3. The comparison of energy consumption in different types CO_2 absorbents

As the measurement of energy consumption for various CO_2 absorbents are often influenced by the simplistic bench-scale equipment, direct comparison of the Q obtained by different researchers becomes challenging. Rui et al. have developed a method to compare the energy consumption of CO_2 absorbents more effectively by normalizing their energy usage against the benchmark of 30 wt% MEA under identical experimental conditions, the concept of relative energy duty (RED) has been introduced for a fair comparison [46].

In this study, we normalized the relative heat duties of 2-PE/APZ-based absorbents by using 5 M MEA as a benchmark and then compared our results with the data from the literature [44,47–51]. The results in Fig. 13 indicate that the relative energy duty (RED) of 2-PE/APZ/DMF (3-2) was only 43 % of the benchmark MEA. The addition of APZ to 2-PE/DMF absorbents reduced their relative energy duty (RED) drastically from 88.7 % to 42.88 %, highlighting the beneficial synergistic effect of 2-PE and APZ in reducing the energy penalty during the regeneration process. 2-PE/APZ-based absorbents offer superior regeneration performance and present themselves as a viable and scalable alternative to MEA in CCS technologies. The specific energy consumption values are available at Table S19.

3.7. The synergistic effect of 2-PE and APZ exploration

The experiment results in the above section reveal a synergistic effect of 2-PE and APZ during CO_2 capture. This beneficial effect promotes absorption and reduces the desorption energy consumption of 2-PE/APZ absorbents. In terms of CO_2 absorption, the synergistic effect increases the CO_2 loading from 0.567 (2-PE/DMF) to 1.004 (2-PE/APZ/DMF) mole CO_2 per mole amine. In terms of CO_2 desorption, the synergistic effect facilitates the full desorption of 2-PE/APZ-based absorbents at 363 K, whereas MEA would necessitate at least 413 K to achieve equivalent desorption efficiency. For exploring the synergistic effect of 2-PE and APZ, In-situ FT-IR, NMR spectroscopy, and DFT calculations are used in the following section [52]. Detailed ¹³C and ¹H NMR spectra are available in the Supporting Information Part 6.

3.7.1. In-situ ATR FT-IR and NMR spectra analysis

The IR spectroscopy is used to analysis the reaction products of the 2-PE/APZ-based absorbents with CO_2 for a time interval of 0, 3, 5, 10, 20, 30 and 40 min to explore the reaction mechanism. Among the 12 of 2-PE/APZ-based absorbents, the 2-PE/DMF, 2-PE/APZ/DMF, 2-PE/APZ/DEGMEE and 2-PE/APZ/EG are selected as the representatives of aprotic solvents, ethers, and glycols for the IR analysis.

For 2-PE/DMF binary absorbents, as shown Fig. 14(a), CO_2 absorption results in four new IR spectrum peaks between 800–1600 cm⁻¹. The peak at 1323 cm⁻¹ suggests carbamate (C-N) formation [53], and it increases with CO_2 absorption. The peaks at 980 and 1180 cm⁻¹ correspond to C-O and C-N stretching, respectively, where 1180 cm⁻¹ is the characteristic peak of 2-PE [54]. A minor peak at 910 cm⁻¹ is likely due to C-N bending or torsions. ¹³C NMR confirms alkyl carbonate and carbamate presence at 163.03 and 160.72 ppm, respectively.

The addition of APZ makes the reaction more complex; several new peaks or shifts at 815, 890, 997, 1280, 1320, and 1564 cm⁻¹ are observed in the IR spectrum. The new peaks are due to the formation of

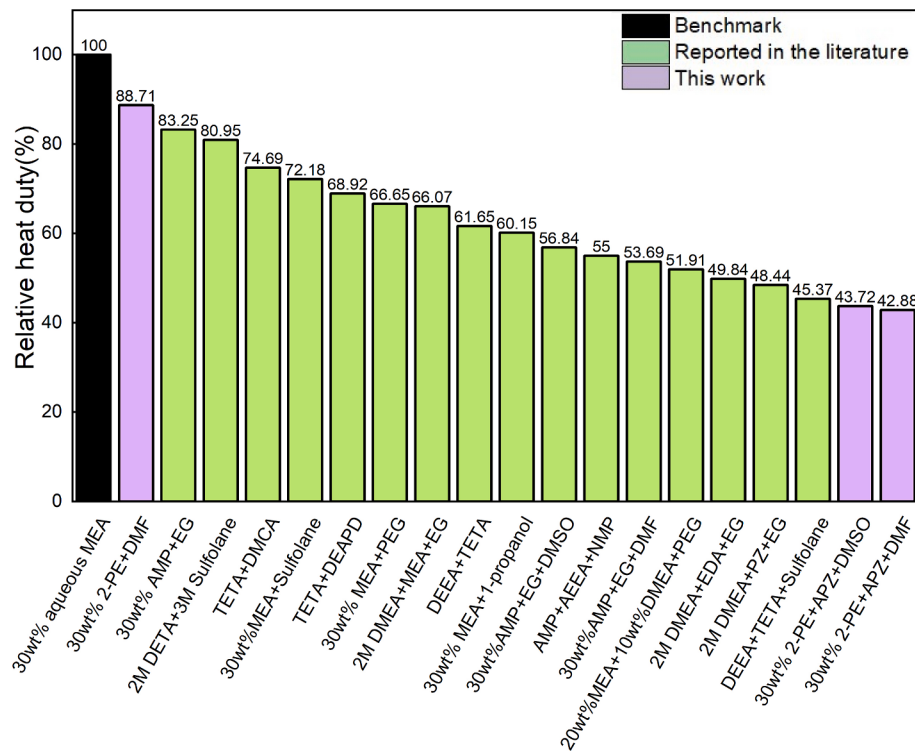


Fig. 13. The relative heat duty (%) of non-aqueous amine-based CO_2 absorbents, with 30 wt% MEA as reference.

new carbamate and carbonate, amine protonation, and molecular CO_2 dissolution. The FT-IR spectrum of 2-PE/APZ/DMF under different CO_2 loading is shown in Fig. 14(b). The 1564 and 1320 cm^{-1} peaks were assigned to asymmetric stretching of COO^- and stretching of $\text{N}-\text{COO}^-$. The 1280 cm^{-1} peak corresponds to the C-O stretching vibrations from carbonate formation. ^{13}C NMR results also confirmed the presence of alkyl carbonate at 162.04 and 159.34 ppm [53]. The minor peaks located at 815 and 890 may be assigned to C-N/C-O bending or torsions. Also, with CO_2 uptake proceeds, the intensity of the 1510 cm^{-1} peak diminishes and then disappears, suggesting N-H depletion on APZ.

2-PE/APZ/DEGMEE and 2-PE/APZ/EG are shown in Fig. 14(c) and (d), demonstrating similar peaks to 2-PE/APZ/DMF but without DMF's masking effects (1640 cm^{-1}). Peaks at 1560 and 1390 cm^{-1} in 2-PE/APZ/DEGMEE relate to COO^- asymmetric and symmetric stretching, indicating APZ-carbamate formation [44]. Peaks at 1290 and 1247 cm^{-1} correspond to $\text{N}-\text{COO}^-$ different stretching vibrations. The shoulder at 1060 cm^{-1} is probably due to the second C-N stretching. For 2-PE/APZ/EG, besides peaks observed in 2-PE/APZ/DEGMEE spectrum, a new peak at 1640 cm^{-1} indicates EG alkyl carbonate ($\text{R}-\text{O}-\text{COO}^-$) formation [53], and confirmed by ^{13}C NMR peak at 158.97 ppm.

3.7.2. Continued ^{13}C NMR for exploring 2-PE and APZ synergistic effect

IR results only confirmed the formation of carbamate and carbonate during CO_2 absorption by 2-PE and APZ but cannot explain their synergistic effect. To explore the synergistic effect and reaction mechanism of 2-PE/APZ-based absorbents, a continued ^{13}C NMR spectroscopy is used to analyse product species at different absorption stages of 2-PE/APZ/DMF (3–2). Fig. 10(a) reveals a two-stage CO_2 absorption process; the peak a (164.25 ppm) is assigned to the characteristic signal of DMF, and the peaks b, c, d, and e collectively signify the presence of carbamate signals in the spectrum. The peak b (163.92 ppm) corresponds to the primary amine carbamate ($\text{NH}-\text{COO}^-$) of APZ, which appears early and intensity increases with CO_2 load but stabilizes after 15 min. Secondary amine carbamate of APZ (signal c at 162.73 ppm) is produced early in the reaction. However, after fifteen minutes of reaction, the intensity of peak c started to increase and shifted to 162.54

ppm, then split into peaks c and d. This indicates the start of the second stage reaction. Simultaneously, peak e (160.74 ppm), representing 2-PE carbamate, shifts to 160.24 ppm, and a minor peak f (158.43 ppm) emerges. This indicates a minor fraction of CO_2 reacting with the hydroxyl group to form carbonate [34].

The 20–60 ppm range corresponds to the C-C bonds region. In Fig. 15 (a) and (c), the peaks g, h, and i signify the propyl, ethyl, and methyl carbons of 2-PE, the shifts of these peaks indicate the protonation to form 2- PEH^+ . After 15 min, peak g and h stabilize, showing 2-PE's protonation ceases, while peak i shifts from 32.04 ppm to 28.10 ppm, it suggested that the presence of carbonate in the neighbouring position. NMR analysis across 20–60 ppm and 158–165 ppm regions shows that APZ's primary amine initially reacts with CO_2 , while 2-PE protonates within the first 15 min. This is first stage CO_2 reaction. Once primary amine of APZ is fully consumed, the secondary amine of APZ dominates the reaction with CO_2 , and APZ's tertiary amine starts to accept the proton transfer. In the meantime, some of 2-PE also reacts CO_2 to form 2-PE carbamate and carbonate. This is evidenced by the stabilization of peaks g and h, and the continued shift of peak I. These reactions belong to second stage CO_2 reaction. This NMR analysis highlights the dynamic interactions and reaction mechanism in CO_2 absorption [34].

To further illustrate the synergistic effect between APZ and 2-PE, the CO_2 was initially injected into 20 wt% APZ-DMF solution, the APZ/DMF quickly became turbid and the separated liquid upper phase and solid lower phase are observed. After adding 1 ml of 2-PE into this two-phase system, the solid phase disappeared instantly, and the solution returned to clearly state. This indicated the redissolution of precipitated substances by 2-PE. The figures of precipitation formed and redissolution are shown in Fig. S12. ^{13}C NMR analysis was performed on fresh APZ-DMF, the liquid upper phase of CO_2 loaded APZ-DMF, and CO_2 loaded APZ-DMF+2-PE. As depicted in Fig. 15(b), there is no detectable CO_2 in the upper phase, which means that all CO_2 is captured in the precipitated phase. However, upon the addition of 2-PE, the liquid turbidity disappeared, and the solid APZ-carbamate dissolved into DMF. As labelled in Fig. 15(c). Peaks 1, 2, and 3 represent APZ and 2-PE carbamates, while shifted peaks 4 and 5 indicate protonated APZ. Thus, in the 2-PE/

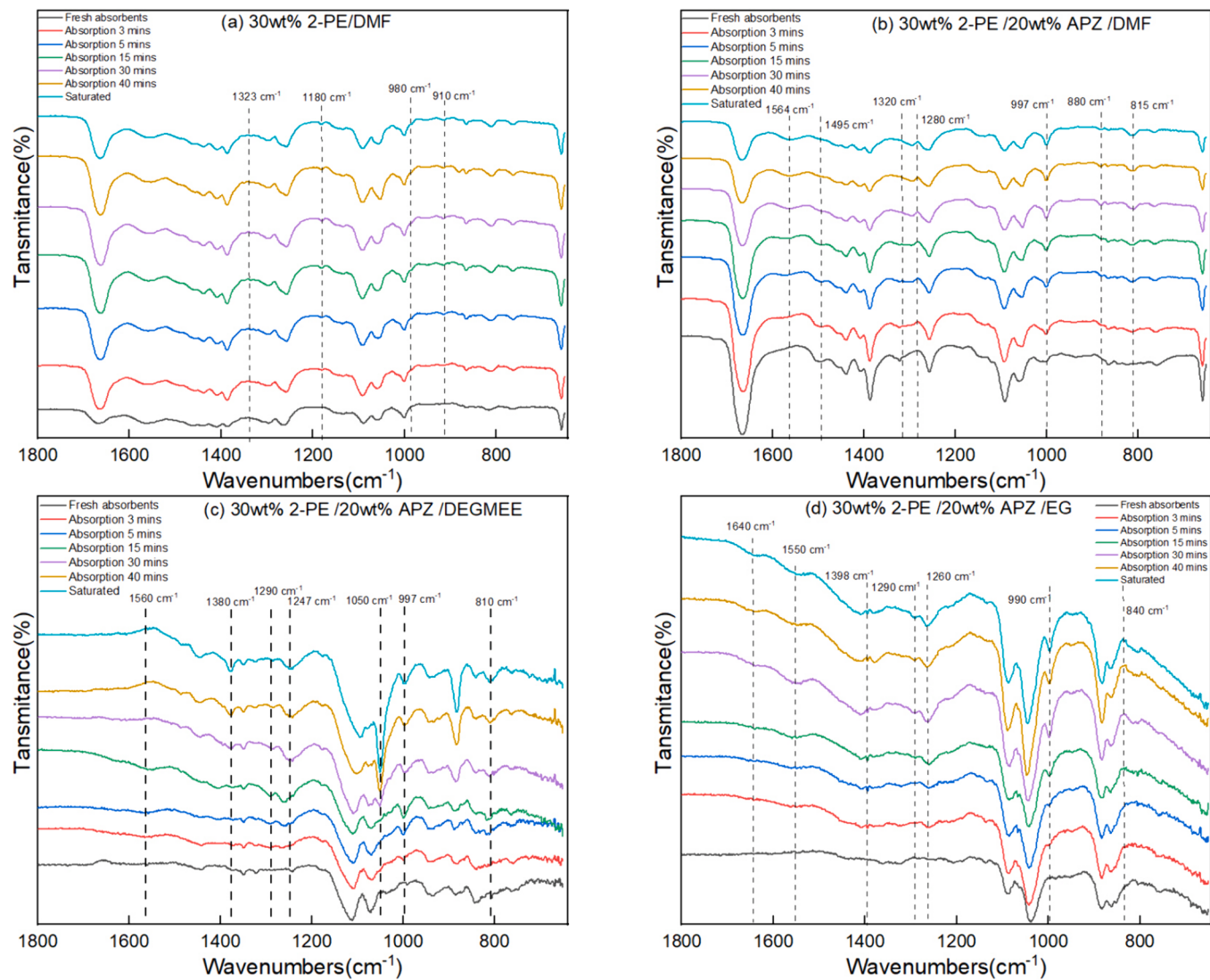


Fig. 14. IR spectrum of 2-PE/APZ-based absorbents (0 min) and after bubbling CO₂ at 3, 5, 15, 30, and 40 min; (a) 2-PE/DMF; (b) 2-PE/APZ/DMF; (c) 2-PE/APZ/DEGMEE; (d) 2-PE/APZ/EG;

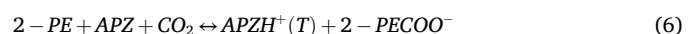
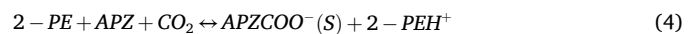
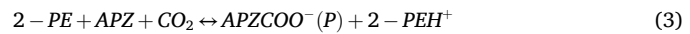
APZ-based absorbents, the APZ could maintain continued high reactivity because 2-PE aids in dissolving solid APZ-carbamate.

3.7.3. DFT calculation for exploring 2-PE and APZ synergistic effect

To delve deeper into the reaction mechanism and the synergistic effect between 2-PE and APZ under CO₂ addition, DFT computational studies were used with the DMol3 module to analyse Gibbs free energy changes (ΔG) and energy barriers. This calculation provided insights into stable molecular structures and formation pathways, indicating the possible reaction pathways, which cannot be provided by the analysis of IR and NMR spectroscopy.

The analysis of CO₂ and proton (H⁺) binding across all amine groups in 2-PE and APZ revealed a total of 12 potential combinations [55]. APZ contains primary amino (P), secondary amino (S), and tertiary amino (T) groups, whereas 2-PE has one sterically hindered amino group (SHA). Computational calculations of energy barriers for various binding combinations helped confirm the sequence of CO₂ absorption on different amine sites, elucidating the complex reaction pathways. This computational work also quantitatively investigates the synergistic effect of 2-PE and APZ by calculating the energy barriers for the following reactions: 2-PE alone reacting with CO₂, APZ alone reacting with CO₂, and the combined reaction of 2-PE and APZ with CO₂.

The possible reactions for CO₂ capture with 2-PE/APZ-based absorbents at the initial stage are:



Their transition state energies and energy barriers were calculated and compared as shown in Fig. 16(a). The energy barrier of reaction is ranked as: 2-PECOO⁻+2-PEH⁺(141.719 kcal/mol) > APZH^{+(T)} + 2-PECOO⁻(117.52 kcal/mol) > APZCOO^{-(S)} + 2-PEH⁺(53.68 kcal/mol) > APZCOO^{-(P)} + 2-PEH⁺(6.88 kcal/mol). The superior low reaction barrier of APZCOO^{-(P)} + 2-PEH⁺ indicated that at the initial CO₂ absorption stage, CO₂ immediately reacts with the primary amine on APZ and transfers a proton to 2-PE, verifying the ¹³C NMR results.

With the CO₂ capture ongoing, the proton transfer site for 2-PE is consumed, and the tertiary amine of APZ begins to receive proton(H⁺), as follows:



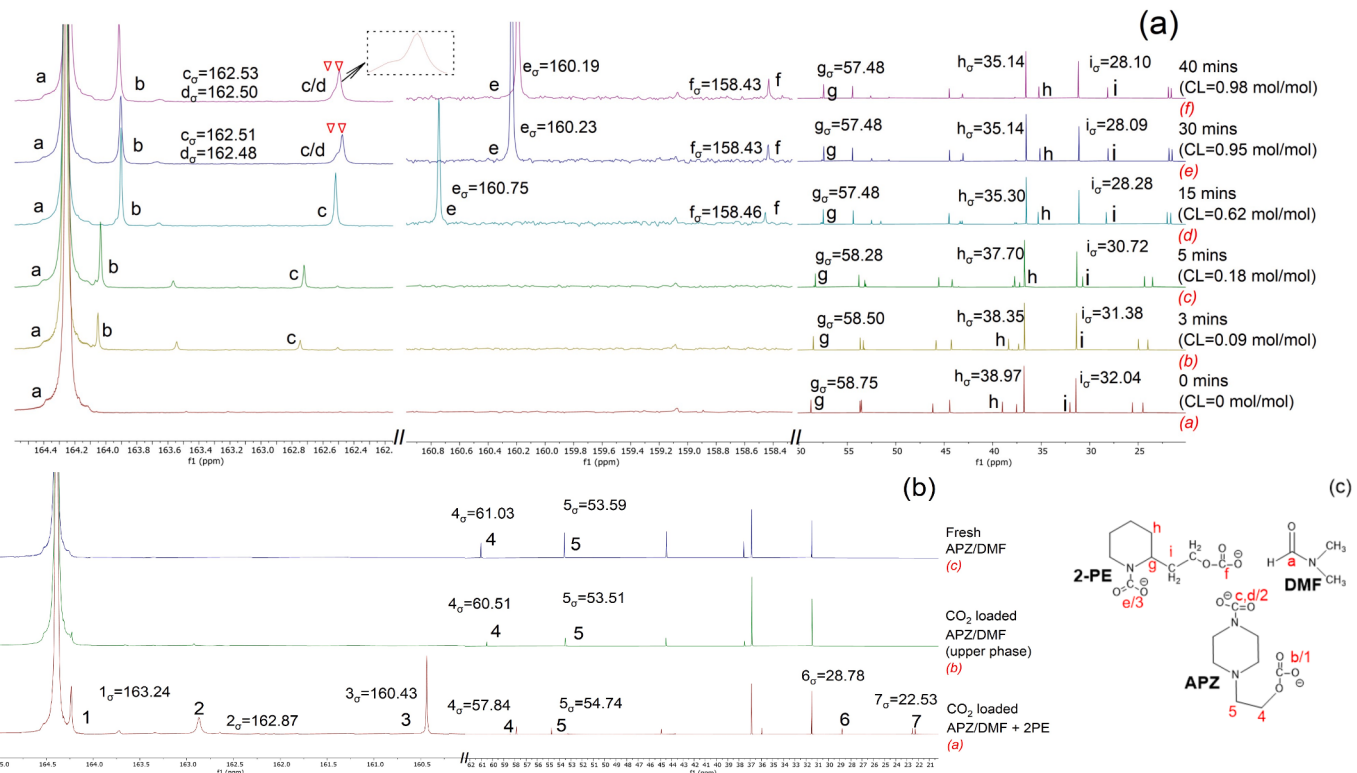


Fig. 15. The ¹³C NMR spectrum analysis: (a) Comparative NMR analysis of 2-PE/APZ/DMF (3–2) absorbents across reaction stages; (b) Comparative NMR analysis of APZ/DMF with and without 2-PE; (c) Labelled molecular structures of 2-PE, APZ and DMF.

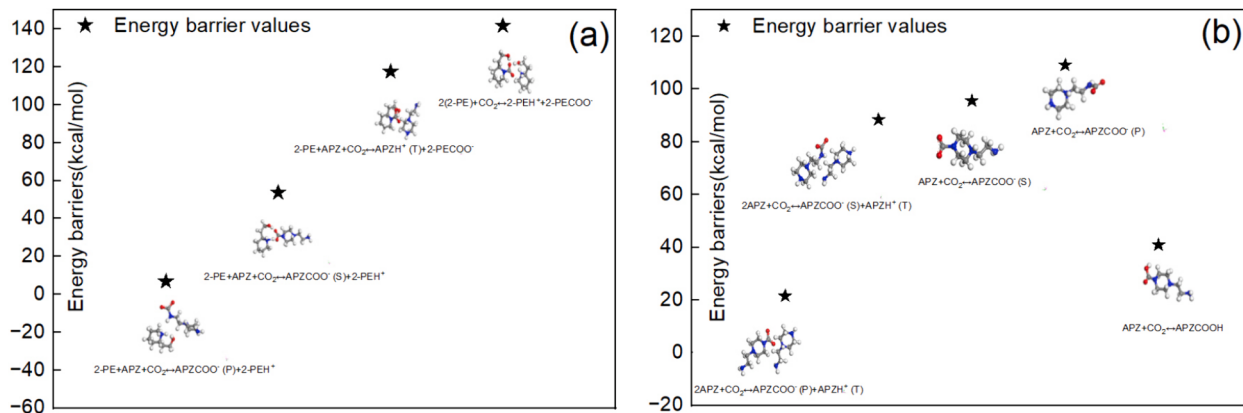


Fig. 16. The energy barriers(kcal/mol) of different products from the reaction of 2-PE/APZ with CO₂; a) Energy barriers of APZH⁺(T) + 2-PECOO⁻, APZCOO⁻(S) + 2-PEH⁺, 2-PECOO⁻+2-PEH⁺, and APZCOO⁻(P) + 2-PEH⁺; b) Energy barriers APZCOO⁻(P) + APZH⁺(T), APZCOO⁻(S) + APZH⁺(T), APZH⁺(T)COO⁻(S), APZH⁺(T)COO⁻(P), and APZCOOH.



The CO₂ can also react with either the primary or secondary amine of APZ. The energy barriers is shown in Fig. 16(b), where APZCOO⁻(S) + APZH⁺(T) (88.37 kcal/mol) > APZCOO⁻(P) + APZH⁺(T) (21.42 kcal/mol). This indicates that in the absence of 2-PE to accept protons, the reaction barrier increased from 6.88 to 21.42 kcal/mol, emphasising the crucial role of 2-PE in enhancing CO₂ absorption.

Moreover, the combination of CO₂ and H⁺ with APZ can lead to three scenarios: binding to the same APZ molecule, binding to different APZ molecules, or forming APZ carbamic acid (APZCOOH):

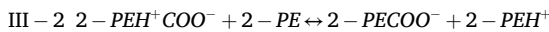
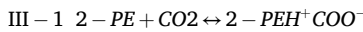
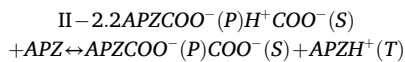
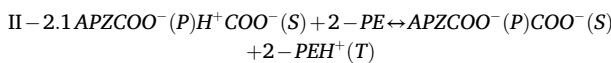
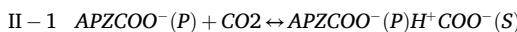
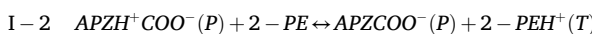
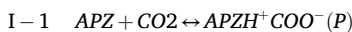


Fig. 16(b) shows higher energy barriers for both COO⁻ and H⁺ reacting on the same APZ molecule at the same time; this indicates the preference for CO₂ and H⁺ binding with different APZ molecules at the same time. Also, the carbamic acid (APZCOOH) also formed in non-aqueous solvents, which is confirmed in previous research [56].

Based on the DFT calculation above, we could quantitatively investigate the synergistic effect of 2-PE and APZ in terms of CO₂ absorption. The reaction barrier of APZCOO⁻(P) + 2-PEH⁺ is only 6.88 kcal/mole, much lower than that of 2-PECOO⁻ + 2-PEH⁺(141.719 kcal/mol) and

$\text{APZCOO}^- + \text{APZH}^+$ (88.37 and 21.42 kcal/mol). This suggests that the synergistic effect between 2-PE and APZ enables them to achieve a significantly high CO_2 absorption rate, promoting the ability to capture CO_2 from the high flow-rate air stream.

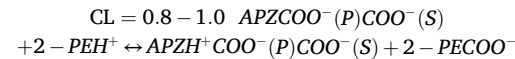
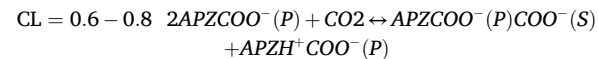
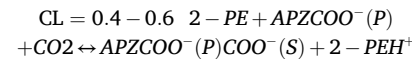
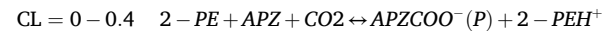
Based on the calculated reaction barriers above, more precise reaction pathways were proposed by utilizing the Gaussian 09 software package. The calculation of the Gibbs free energy (ΔG) for reactants, products, and transition states pinpointed the reaction pathways of 2-PE/APZ-based absorbents with CO_2 . The entire DFT calculation was performed within DMF solvent model to simulate a real reaction and adopted a zwitterion mechanism as its basis [57]. Fig. 17 showcases transition state molecules and three reaction paths, which are labelled I, II and III. In these reactions, the I-1, II-1 and III-1 belong to the zwitterion formed by amino groups and CO_2 . The reaction I-2, II-2.1, II-2.2 and III-2 are the process of zwitterion deprotonation to form the carbamate. The activation free energies and Gibbs free energy changes for these pathways are comprehensively summarized in Table S10.



The pathways I and II show that zwitterion formation from 2-PE/APZ and CO_2 is the rate-limiting step, as the ΔG changes for zwitterion generation (5.637 KJ/mol) surpasses the energy for zwitterion deprotonation (1.837 KJ/mol). The activation energy required for APZCOO^- (II-1) is 5.60 times higher than that of APZ (I-1) to generate the zwitterion. This could explain the instantaneous decrease in the CO_2 absorption rate with CO_2 capture processed as shown in Section 3.2. After zwitterion formation, the zwitterion deprotonations (I-2, II-2.1, II-2.2 and III-2) were easy to occur because they were nonactivation-free energy processes. The synergistic effect of 2-PE and APZ is further evident

when examining the reaction pathways, particularly in comparison to pathways I and III. The activation energy required for the formation of 2-PE zwitterion (9.648 KJ/mol) is higher than that for APZ zwitterion (5.637 KJ/mol), indicating APZ's superior reactivity with CO_2 . Also, the free energy changes showed that the deprotonation process of 2-PE/APZ zwitterion is much easier than single 2-PE zwitterion. This synergistic effect leads to the superior CO_2 capture ability of 2-PE/APZ-based absorbents.

In summary, based on theoretical and experimental results, the following conclusions can be drawn. Firstly, the reaction mechanisms of CO_2 with 2-PE/APZ-based absorbents varied with the CO_2 loading. The equations below show the reactions at the different CO_2 absorption stages, where CL means CO_2 loading. For example, when CL ranges from 0 to 0.4, the primary amine of APZ and 2-PE dominated the CO_2 absorption. Secondly, the synergistic effect of 2-PE and APZ is quantitatively clarified, especially how this effect enhances the CO_2 absorption kinetics. This effect enables the 2-PE/APZ-based absorbents to capture CO_2 from high flow-rate air.



3.7.4. The CO_2 desorption mechanism of 2-PE/APZ

For exploring the synergistic effect between 2-PE and APZ in terms of desorption performance, IGMH analysis based on Hirshfeld density was used to investigate the interaction forces among the chemical species present in the products at different stages of CO_2 absorption [38].

As illustrated in Fig. 18, the color-coded regions showed distinct interactions within the product molecules, where the blue region (-0.05 to -0.02) is for strong attractions (e.g., hydrogen bonding) with high electron cloud density, the green region (-0.02 to 0.02) denotes van der Waals attractions with moderate electron cloud density, and the red region (0.02 to 0.05) for steric hindrance effects with positive electron cloud density. IGMH analysis (Fig. 18(a)) showed the weakest interaction between 2-PE and APZ without CO_2 absorption. The addition of CO_2

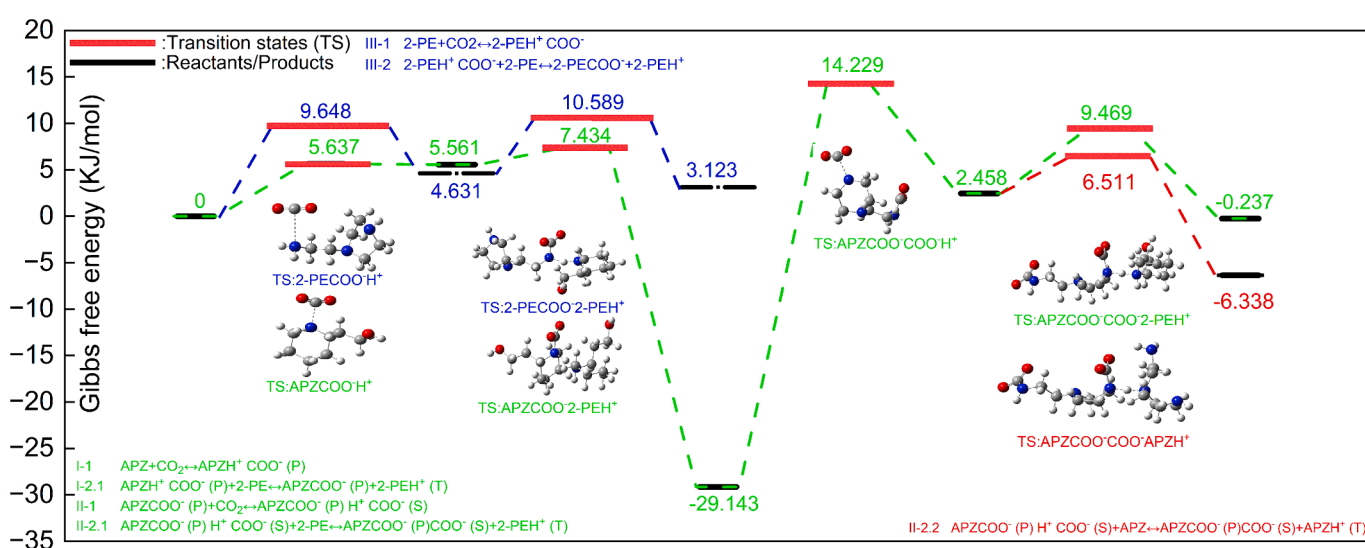


Fig. 17. Schematic of Gibbs free energy surface for CO_2 absorption into 2-PE/APZ/DMF absorbent. The green line, blue line, and red line present the pathway I, II and III respectively. (For interpretation of the references to color in this figure legend, the reader is referred to the web version of this article.)

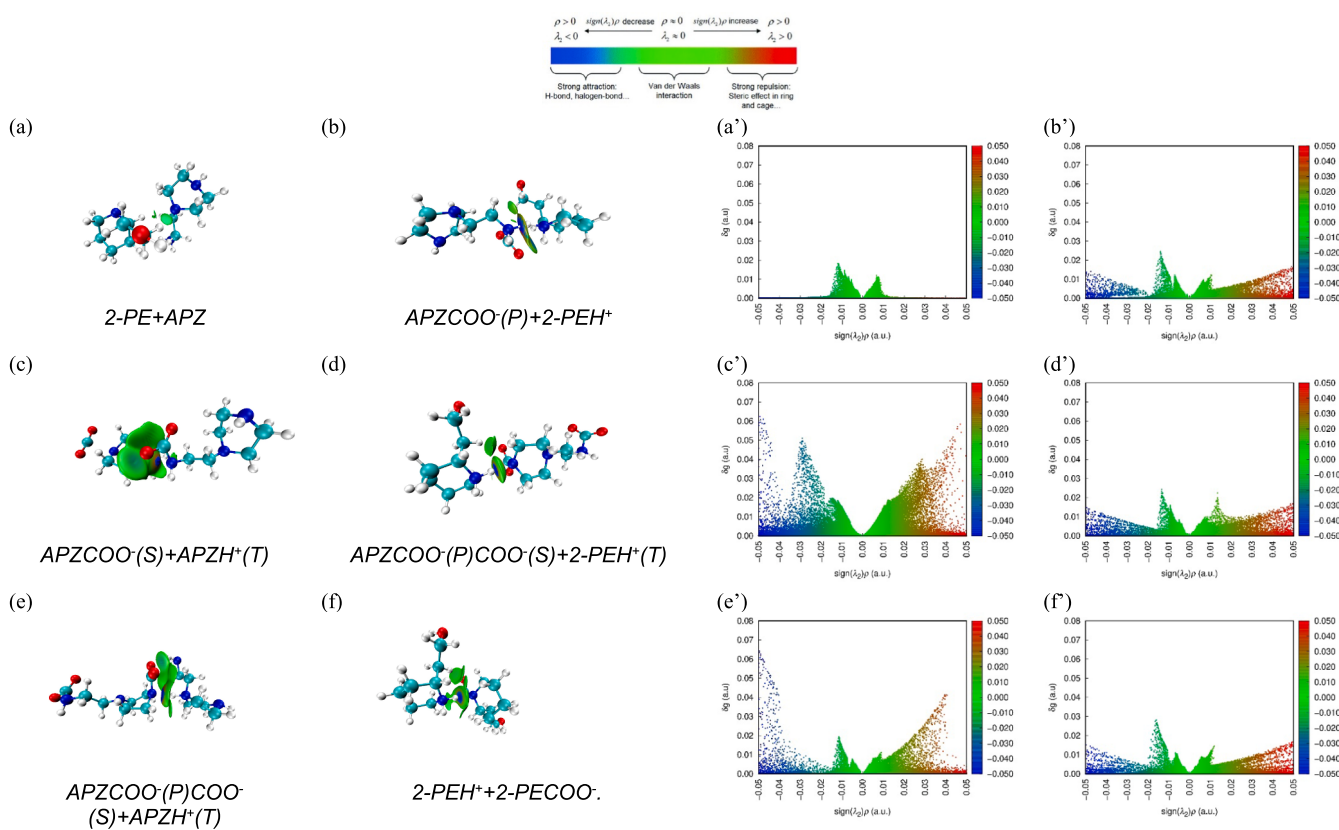


Fig. 18. The IGMH iso-surface (left) and scatter (right) analysis showing weak interaction between the absorption products, which corresponds to the diagrams on the right-hand side with the same numbers. (a) 2-PE+APZ; (b) APZCOO^(P) + 2-PEH⁺; (c) APZCOO^(S) + APZH^(T); (d) APZCOO^(P) COO^(S) + 2-PEH^(T); (e) APZCOO^(P) COO^(S) + APZH^(T); (f) 2-PEH⁺+2-PECOO⁻.

resulted in a strong interaction (hydrogen bonding and vdW forces) among amine-CO₂ complex.

Fig. 18(c), (e) show the interactions between APZCOO⁻ and APZH⁺ systems as well as between APZCOO⁻COO⁻ and APZH⁺. Fig. 18(b), (d), and (f) show the interaction between APZCOO⁻ and 2-PEH⁺, APZCOO⁻COO⁻ and 2-PEH⁺, as well as 2-PECOO⁻ and 2-PEH⁺. These results reveal how intermolecular forces vary in different 2-PE/APZ reaction systems. The dramatically increased density in the blue region of the right side scatter graphs for Fig. 18(c) and (e) over Fig. 18(b), (d), and (f) indicate that 2-PE effectively reduces the attractive forces between amine-CO₂ products [34]. The reduced attractive forces due to the 2-PEH⁺ formed ion pairs with APZCOO⁻, which effectively weaken the intermolecular interaction.

This observation implies that the presence of 2-PE plays a crucial role in altering the intermolecular interactions, particularly in diminishing the hydrogen bonding and vdW forces between 2-PEH⁺/APZCOO⁻ complex. Therefore, the synergistic effect between 2-PE and APZ facilitates their low-temperature regeneration capability while possessing high absorption performance.

3.7.5. Summary of absorption/desorption mechanism for 2-PE/APZ-based absorbents

In this section, the synergistic effect between 2-PE and APZ have been thoroughly investigated theoretically and experimentally. Based on this effect, the CO₂ absorption mechanism by 2-PE/APZ-based absorbents are proposed. The single 2-PE or APZ showed inadequate CO₂ capture ability, while the combination of 2-PE and APZ could enhance the CO₂ capture performance significantly.

For the 2-PE/DMF binary absorbent, CO₂ absorption follows the zwitterion mechanism, in which CO₂ firstly reacts with 2-PE forming 2-PE zwitterion(2-PEH⁺COO⁻), then followed by the deprotonation of

zwitterion to 2-PE carbamate. However, due to the weak affinity between 2-PE and CO₂, this reaction rate is slow. The absorption capacity of 2-PE/DMF is 58.7 (g-CO₂/kg-soln.), which is only 48.7 % of MEA-H₂O's capacity under the same conditions. For the APZ/DMF binary absorbent, a formed APZ zwitterion (APZH⁺COO⁻) precipitated during CO₂ absorption, halting the reaction.

When 2-PE and APZ are combined for CO₂ capture, CO₂ initially reacts with APZ to rapidly form an APZ zwitterion, followed by deprotonation to 2-PE. This combination of 2-PE and APZ allows for proton transfer and carbamate formation on separate amines in the system, where 2-PEH⁺ ion pairs with APZCOO⁻, reducing the hydrogen bonding and vdW attraction in the amine-CO₂ complex. The reduced attraction prevents the precipitation of APZ zwitterion (APZH⁺COO⁻) maintaining the APZ with high reactivity. Based on DFT calculation, the synergistic effect of 2-PE and APZ are quantitatively explained. As a result, this synergistic effect promotes the increase of 191.8 % in the CO₂ absorption capacity from 58.7 to 171.3 (g-CO₂/kg-soln.), with CO₂ loading reaching 1.004 mol CO₂/mole amine. The superior CO₂ absorption kinetics enables it to remove CO₂ from the high flow-rate air.

Similarly, the weak ion pairs formed by 2-PEH⁺ and APZCOO⁻ also facilitate CO₂ desorption at a lower temperature. For 2-PE/APZ/DMF, 2-PE/APZ/DMSO, and 2-PE/APZ/NMF, the desorption efficiency at 363 K reached 91.41 %, 89.22 %, and 88.15 %, respectively, resulting in 157.24, 132.40 and 128.99 (g-CO₂/kg-soln.) released. In contrast, the MEA-H₂O desorbed only 103.2 (g-CO₂/kg-soln.) at the same temperature.

The synergistic effect of the 2-PE and APZ addressed the challenges in applying non-aqueous absorbents for direct air capture. The reaction mechanism and routes are summarized in Fig. 19.

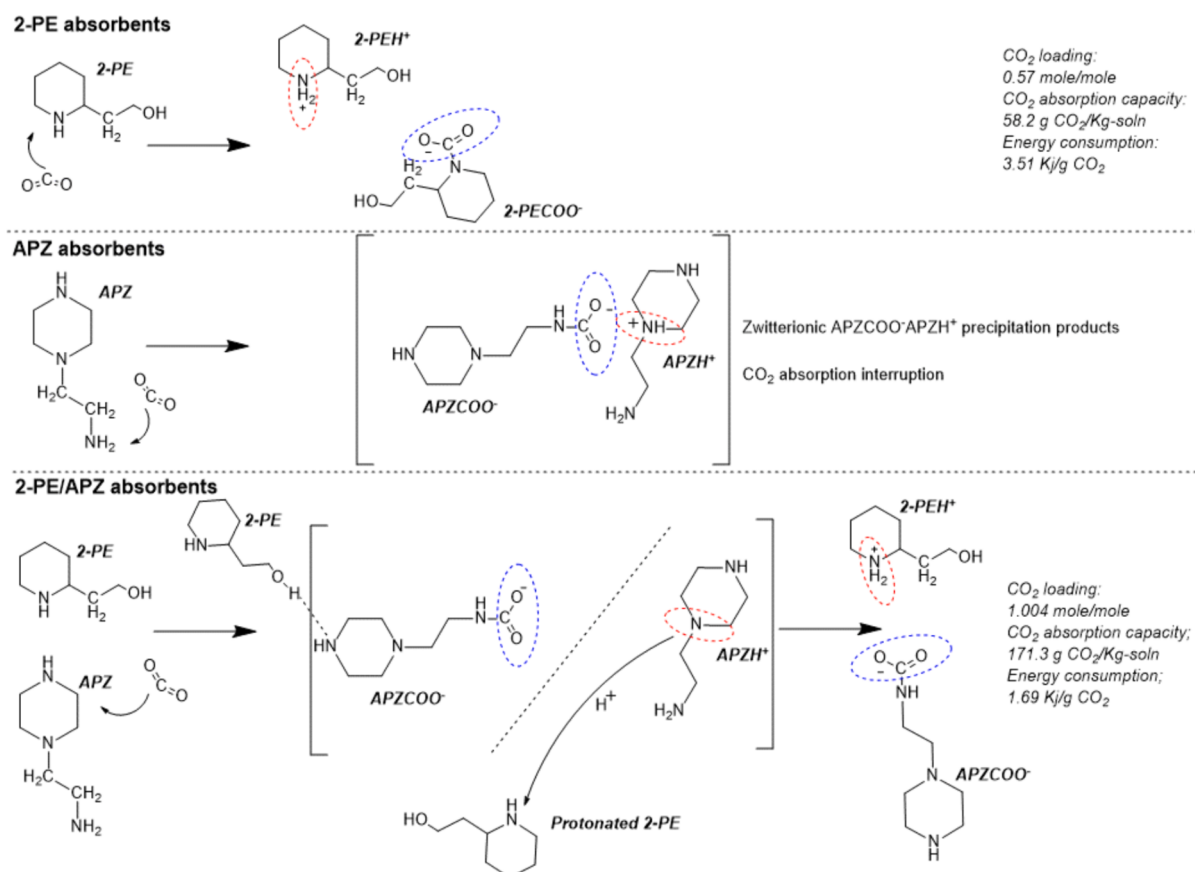


Fig. 19. The reaction routes between 2-PE with CO₂, APZ with CO₂ and 2-PE/APZ with CO₂.

4. Conclusion

Energy-efficient 2-PE/APZ-based absorbents with high CO₂ capture performance have been developed through a solvent screening strategy based on MD simulation. These novel absorbents can effectively capture CO₂ from both flue gas and air, showcasing their ability to handle ultra-dilute CO₂ streams. Six different solvents were screened and tested in this 2-PE/APZ system, including aprotic solvents (DMF, DMSO and NMF), ether (DEGMEE), glycol (EG) and water. The results showed that aprotic solvents enhanced the carbon capture performance of 2-PE/APZ-based absorbents, while EG weakened it. The effectiveness of 2-PE/APZ absorbents in capturing CO₂ is intrinsically linked to the solvation free energies of amine-CO₂ products in various solvents, which is proved through DFT calculation. Among these absorbents, 2-PE/APZ/DMF shows the best performance with the CO₂ loading of 1.004 mol/mole, reaching the theoretical maximum. In 24 h continued DAC experiments, a total of 87.31 % of CO₂ was captured from the air, and the regeneration heat duty was decreased to 1.694 MJ/t CO₂, which was 55.89 % lower than that of MEA-H₂O. Moreover, these 2-PE/APZ-based absorbents demonstrate great recyclability and thermal stability. After five absorption-desorption cycles, the CO₂ loading remained at 0.942 with a regeneration efficiency of 90.38 %. Based on DFT calculation, IR and NMR spectroscopy, the reaction mechanism and synergistic effect of 2-PE and APZ were systematically investigated. In 2-PE and APZ mixture, CO₂ rapidly reacts with APZ, leading to the formation of APZ zwitterion. Subsequently, deprotonation on 2-PE occurs, leading to the formation of 2-PEH⁺ and APZCOO⁻ ion pairs and 2-PE could significantly reduce the vdW and hydrogen-bonding forces in the amine-CO₂ complex. The reduced attraction effectively maintains the high reactivity of APZ and prevents the precipitation of APZ zwitterion (APZH⁺COO⁻), which is verified by DFT calculation and IGMH analysis. As a result, the synergistic effect of 2-PE and APZ enables them to

effectively capture CO₂ from air, and CO₂ absorption capacity increased by 191.8 % compared to 2-PE/DMF. Therefore, the developed 2-PE/APZ-based absorbents open new avenues for advancing next-generation amine absorbents for commercial applications in CO₂ capture.

CRediT authorship contribution statement

Guanchu Lu: Writing – review & editing, Writing – original draft, Visualization, Software, Resources, Methodology, Investigation, Formal analysis, Data curation. **Zongyang Yue:** Writing – review & editing. **Yanan Deng:** Writing – review & editing. **Yuxiang Xue:** Resources. **Yi Huang:** Supervision. **Xiaolei Zhang:** Supervision, Software. **Xianfeng Chen:** Writing – review & editing, Supervision, Project administration, Funding acquisition, Formal analysis, Conceptualization. **Xianfeng Fan:** Writing – review & editing, Supervision, Project administration, Funding acquisition, Formal analysis, Conceptualization.

Declaration of competing interest

The authors declare that they have no known competing financial interests or personal relationships that could have appeared to influence the work reported in this paper.

Data availability

Data will be made available on request.

Appendix A. Supplementary data

Supplementary data to this article can be found online at <https://doi.org/10.1016/j.cej.2024.154085>.

References

- [1] J. Godin, W. Liu, S. Ren, C.C. Xu, Advances in recovery and utilization of carbon dioxide: A brief review, *J. Environ. Chem. Eng.* 9 (4) (2021) 105644, <https://doi.org/10.1016/j.jece.2021.105644>.
- [2] X. (Eric) Hu, et al., A review of N-functionalized solid adsorbents for post-combustion CO₂ capture, *Appl. Energy* 260 (2020) 114244, <https://doi.org/10.1016/j.apenergy.2019.114244>.
- [3] G. Lu, Z. Wang, U.H. Bhatti, X. Fan, "recent Progress in Carbon Dioxide Capture Technologies : A Review" 1 (1) (2023) pp, <https://doi.org/10.18686/cest.v1i1.32>.
- [4] S. Kikkawa, et al., Direct Air Capture of CO₂ Using a Liquid Amine-Solid Carbamic Acid Phase-Separation System Using Diamines Bearing an Aminocyclohexyl Group, *ACS Environ. Au* 2 (4) (Jul. 2022) 354–362, <https://doi.org/10.1021/acsenvironau.1c00065>.
- [5] L. Liu, et al., Low-cost DETA impregnation of acid-activated sepiolite for CO₂ capture, *Chem. Eng. J.* 353 (2018) 940–948, <https://doi.org/10.1016/j.cej.2018.07.086>.
- [6] R. Idem, et al., Pilot Plant Studies of the CO₂ Capture Performance of Aqueous MEA and Mixed MEA/MDEA Solvents at the University of Regina CO₂ Capture Technology Development Plant and the Boundary Dam CO₂ Capture Demonstration Plant, *Ind. Eng. Chem. Res.* 45 (8) (Apr. 2006) 2414–2420, <https://doi.org/10.1021/ie050569e>.
- [7] K. Fu, W. Rongwong, Z. Liang, Y. Na, R. Idem, P. Tontiwachwuthikul, Experimental analyses of mass transfer and heat transfer of post-combustion CO₂ absorption using hybrid solvent MEA-MeOH in an absorber, *Chem. Eng. J.* 260 (Jan. 2015) 11–19, <https://doi.org/10.1016/j.cej.2014.08.064>.
- [8] S. Chen, S. Chen, Y. Zhang, L. Qin, C. Guo, J. Chen, Species distribution of CO₂ absorption/desorption in aqueous and non-aqueous N-ethylmonoethanolamine solutions, *Int. J. Greenh. Gas Control* 47 (Apr. 2016) 151–158, <https://doi.org/10.1016/J.IJGGC.2016.01.046>.
- [9] C. Guo, S. Chen, Y. Zhang, G. Wang, Solubility of CO₂ in nonaqueous absorption system of 2-(2-aminoethylamine)ethanol + benzyl alcohol, *J. Chem. Eng. Data* 59 (6) (Jun. 2014) 1796–1801, https://doi.org/10.1021/JE401028G/ASSET/IMAGES/MEDIUM/JE-2013-01028G_0010.GIF.
- [10] I.I.I. Alkhaitib, L.M.C. Pereira, A. Alhajai, L.F. Vega, Performance of non-aqueous amine hybrid solvents mixtures for CO₂ capture: A study using a molecular-based model, *J. CO₂ Util.* 35 (Jan. 2020) 126–144, <https://doi.org/10.1016/J.JCOU.2019.09.010>.
- [11] J. Tan, H. Shao, J. Xu, L. Du, G. Luo, Mixture Absorption System of Monoethanolamine-Triethylene Glycol for CO₂ Capture, *Ind. Eng. Chem. Res.* 50 (7) (Apr. 2011) 3966–3976, <https://doi.org/10.1021/IE101810A>.
- [12] J. Li, C. You, L. Chen, Y. Ye, Z. Qi, K. Sundmacher, Dynamics of CO₂ Absorption and Desorption Processes in Alkanolamine with Cosolvent Polyethylene Glycol, *Ind. Eng. Chem. Res.* 51 (37) (Sep. 2012) 12081–12088, <https://doi.org/10.1021/IE301164V>.
- [13] C.H. Yu, T.W. Wu, C.S. Tan, CO₂ capture by piperazine mixed with non-aqueous solvent diethylene glycol in a rotating packed bed, *Int. J. Greenh. Gas Control* 19 (Nov. 2013) 503–509, <https://doi.org/10.1016/J.IJGGC.2013.10.014>.
- [14] C. Zheng, J. Tan, Y.J. Wang, G.S. Luo, CO₂ Solubility in a Mixture Absorption System of 2-Amino-2-methyl-1-propanol with Glycol, *Ind. Eng. Chem. Res.* 51 (34) (Aug. 2012) 11236–11244, <https://doi.org/10.1021/IE3007165>.
- [15] T. Ping, Y. Dong, S. Shen, Energy-Efficient CO₂Capture Using Nonaqueous Absorbents of Secondary Alkanolamines with a 2-Butoxyethanol Cosolvent, *ACS Sustain. Chem. Eng.* 8 (49) (Dec. 2020) 18071–18082, https://doi.org/10.1021/ACSSUSCHEMENG.0C06345/SUPPL_FILE/SC0C06345_SI_001.PDF.
- [16] F. Bougie, D. Pokras, X. Fan, Novel non-aqueous MEA solutions for CO₂ capture, *Int. J. Greenh. Gas Control* 86 (Jul. 2019) 34–42, <https://doi.org/10.1016/j.ijggc.2019.04.013>.
- [17] F. Barzagli, C. Giorgi, F. Mani, M. Peruzzini, Reversible carbon dioxide capture by aqueous and non-aqueous amine-based absorbents: A comparative analysis carried out by 13C NMR spectroscopy, *Appl. Energy* 220 (March) (2018) 208–219, <https://doi.org/10.1016/j.apenergy.2018.03.076>.
- [18] H. Guo, C. Li, X. Shi, H. Li, S. Shen, Nonaqueous amine-based absorbents for energy efficient CO₂ capture, *Appl. Energy* 239 (Apr. 2019) 725–734, <https://doi.org/10.1016/j.apenergy.2019.02.019>.
- [19] K. Fu, C. Liu, L. Wang, X. Huang, D. Fu, Performance and mechanism of CO₂ absorption in 2-ethylhexan-1-amine + glyme non-aqueous solutions, *Energy* 220 (Apr. 2021) 119735, <https://doi.org/10.1016/J.ENERGY.2020.119735>.
- [20] L. Bihong, Y. Kexuan, Z. Xiaobin, Z. Zuoming, J. Guohua, 2-Amino-2-methyl-1-propanol based non-aqueous absorbent for energy-efficient and non-corrosive carbon dioxide capture, *Appl. Energy* 264 (Apr. 2020), <https://doi.org/10.1016/j.apenergy.2020.114703>.
- [21] H. Svensson, J. Edfeldt, V. Zejnullah Velasco, C. Hulteberg, H.T. Karlsson, Solubility of carbon dioxide in mixtures of 2-amino-2-methyl-1-propanol and organic solvents, *Int. J. Greenh. Gas Control* 27 (Aug. 2014) 247–254, <https://doi.org/10.1016/J.IJGGC.2014.06.004>.
- [22] Y. Li, J. Cheng, L. Hu, J. Liu, J. Zhou, and K. Cen, "Phase-changing solution PZ/DMF for efficient CO₂ capture and low corrosiveness to carbon steel," *Fuel*, vol. 216, no. December 2017, pp. 418–426, 2018, doi: 10.1016/j.fuel.2017.12.030.
- [23] X. Gao, X. Li, S. Cheng, B. Lv, G. Jing, Z. Zhou, A novel solid-liquid 'phase controllable' biphasic amine absorbent for CO₂ capture, *Chem. Eng. J.* 430 (Feb. 2022) 132932, <https://doi.org/10.1016/J.CEJ.2021.132932>.
- [24] F. Barzagli, F. Mani, M. Peruzzini, Novel water-free biphasic absorbents for efficient CO₂ capture, *Int. J. Greenh. Gas Control* 60 (2017) 100–109, <https://doi.org/10.1016/j.ijggc.2017.03.010>.
- [25] F. Barzagli, C. Giorgi, F. Mani, M. Peruzzini, Comparative Study of CO₂ Capture by Aqueous and Nonaqueous 2-Amino-2-methyl-1-propanol Based Absorbents Carried Out by 13C NMR and Enthalpy Analysis, *Ind. Eng. Chem. Res.* 58 (11) (2019) 4364–4373, <https://doi.org/10.1021/acs.iecr.9b00552>.
- [26] F. Barzagli, C. Giorgi, F. Mani, M. Peruzzini, Screening Study of Different Amine-Based Solutions as Sorbents for Direct CO₂ Capture from Air, *ACS Sustain. Chem. Eng.* 8 (37) (Sep. 2020) 14013–14021, <https://doi.org/10.1021/acssuschemeng.0c03800>.
- [27] F. Barzagli, C. Giorgi, F. Mani, M. Peruzzini, Reversible carbon dioxide capture by aqueous and non-aqueous amine-based absorbents: A comparative analysis carried out by 13C NMR spectroscopy, *Appl. Energy* 220 (January) (2018) 208–219, <https://doi.org/10.1016/j.apenergy.2018.03.076>.
- [28] D. Wei, et al., Kinetic study on CO₂ absorption by aqueous secondary amine + tertiary amine blends: Kinetic model and effect of the chain length of tertiary amine, *Chem. Eng. Sci.* 292 (2024) 119996, <https://doi.org/10.1016/j.ces.2024.119996>.
- [29] D. Yang, M. Lv, J. Chen, Efficient non-aqueous solvent formed by 2-piperidinethanol and ethylene glycol for CO₂ absorption, *Chem. Commun.* 55 (83) (2019) 12483–12486, <https://doi.org/10.1039/c9cc06320j>.
- [30] F. Bougie, X. Fan, Microwave regeneration of monoethanolamine aqueous solutions used for CO₂ capture, *Int. J. Greenh. Gas Control* 79 (July) (2018) 165–172, <https://doi.org/10.1016/j.ijggc.2018.10.008>.
- [31] F. Bougie, X. Fan, Analysis of the Regeneration of Monoethanolamine Aqueous Solutions by Microwave Irradiation, *Energy Procedia* 142 (2017) 3661–3666, <https://doi.org/10.1016/j.egypro.2017.12.259>.
- [32] Z. Liang, R. Idem, P. Tontiwachwuthikul, F. Yu, H. Liu, W. Rongwong, Experimental study on the solvent regeneration of a CO₂-loaded MEA solution using single and hybrid solid acid catalysts, *AIChE J.* 62 (3) (Mar. 2016) 753–765, <https://doi.org/10.1002/aic.15073>.
- [33] G. Jing, Y. Qian, X. Zhou, B. Lv, Z. Zhou, Designing and Screening of Multi-Amino-Functionalized Ionic Liquid Solution for CO₂ Capture by Quantum Chemical Simulation, *ACS Sustain. Chem. Eng.* 6 (1) (Jan. 2018) 1182–1191, <https://doi.org/10.1021/acssuschemeng.7b03467>.
- [34] X. Gao, X. Li, S. Cheng, B. Lv, G. Jing, Z. Zhou, A novel solid-liquid 'phase controllable' biphasic amine absorbent for CO₂ capture, *Chem. Eng. J.* 430 (2022) 132932, <https://doi.org/10.1016/j.cej.2021.132932>.
- [35] M.J. Frisch, et al., "G16_C01". p, Gaussian 16, Revision C.01, Gaussian Inc, Wallin (2016).
- [36] M.J. Al-Marri, M.M. Khader, E.P. Giannelis, M.F. Shibli, Optimization of selection of chain amine scrubbers for CO₂ capture, *J. Mol. Model.* 20 (12) (2014) 2518, <https://doi.org/10.1007/s00894-014-2518-8>.
- [37] X. Li, et al., Low energy-consuming CO₂ capture by phase change absorbents of amine/alcohol/H₂O, *Sep. Purif. Technol.* 275 (2021) 119181, <https://doi.org/10.1016/j.seppur.2021.119181>.
- [38] T. Lu, Q. Chen, Independent gradient model based on Hirshfeld partition: A new method for visual study of interactions in chemical systems, *J. Comput. Chem.* 43 (8) (Mar. 2022) 539–555, <https://doi.org/10.1002/jcc.26812>.
- [39] T. Lu, F. Chen, Multiwfns: A multifunctional wavefunction analyzer, *J. Comput. Chem.* 33 (5) (Feb. 2012) 580–592, <https://doi.org/10.1002/jcc.22885>.
- [40] S. Zhang Y. Shen L. Wang J. Chen Y. Lu Phase change solvents for post-combustion CO₂ capture: Principle, advances, and challenges *Appl. Energy* 239 November 2019 2018, pp. 876–897 10.1016/j.apenergy.2019.01.242.
- [41] Y. Song P.G. Ranjith B. Wu Development and experimental validation of a computational fluid dynamics-discrete element method sand production model *J. Nat. Gas Sci. Eng.* 73 July 2020 2019, p. 103052 10.1016/j.jngse.2019.103052.
- [42] W. Tian, et al., Nonaqueous MEA/PEG200 Absorbent with High Efficiency and Low Energy Consumption for CO₂ Capture, *Ind. Eng. Chem. Res.* 60 (10) (Mar. 2021) 3871–3880, <https://doi.org/10.1021/acs.iecr.0c05294>.
- [43] C. Nwaoha, et al., Advancement and new perspectives of using formulated reactive amine blends for post-combustion carbon dioxide (CO₂) capture technologies, *Petroleum* 3 (1) (2017) 10–36, <https://doi.org/10.1016/j.petlm.2016.11.002>.
- [44] G. Lu, et al., Development of novel AMP-based absorbents for efficient CO₂ capture with low energy consumption through modifying the electrostatic potential, *Chem. Eng. J.* 474 (2023) 145929, <https://doi.org/10.1016/j.cej.2023.145929>.
- [45] X. Zhu, et al., DBU-Glycerol Solution: A CO₂Absorbent with High Desorption Ratio and Low Regeneration Energy, *Environ. Sci. Technol.* 54 (12) (2020) 7570–7578, <https://doi.org/10.1021/acs.est.0c01332>.
- [46] X. He, H. He, F. Barzagli, M.W. Amer, C. Li, R. Zhang, Analysis of the energy consumption in solvent regeneration processes using binary amine blends for CO₂ capture, *Energy* 270 (2023) 126903, <https://doi.org/10.1016/j.energy.2023.126903>.
- [47] L. Wang, S. Yu, Q. Li, Y. Zhang, S. An, S. Zhang, Performance of sulfolane/DETA hybrids for CO₂ absorption: Phase splitting behavior, kinetics and thermodynamics, *Appl. Energy* 228 (2018) 568–576, <https://doi.org/10.1016/j.apenergy.2018.06.077>.
- [48] R. Wang, L. Jiang, Q. Li, G. Gao, S. Zhang, L. Wang, Energy-saving CO₂ capture using sulfolane-regulated biphasic solvent, *Energy* 211 (2020) 118667, <https://doi.org/10.1016/j.energy.2020.118667>.
- [49] S. Zhang, Y. Shen, P. Shao, J. Chen, L. Wang, Kinetics, Thermodynamics, and Mechanism of a Novel Biphasic Solvent for CO₂ Capture from Flue Gas, *Environ. Sci. Technol.* 52 (6) (Mar. 2018) 3660–3668, <https://doi.org/10.1021/acs.est.7b05936>.
- [50] L. Wang, et al., Advanced Monoethanolamine Absorption Using Sulfolane as a Phase Splitter for CO₂ Capture, *Environ. Sci. Technol.* 52 (24) (2018) 14556–14563, <https://doi.org/10.1021/acs.est.8b05654>.

- [51] L. Wang, S. Liu, R. Wang, Q. Li, S. Zhang, Regulating Phase Separation Behavior of a DEEA-TETA Biphasic Solvent Using Sulfolane for Energy-Saving CO₂ Capture, Environ. Sci. Technol. 53 (21) (Nov. 2019) 12873–12881, <https://doi.org/10.1021/acs.est.9b02787>.
- [52] X.E. Hu, et al., NMR Techniques and Prediction Models for the Analysis of Species Formed in CO₂ Capture Processes with Amine-Based Sorbents: A Critical Review, ACS Sustain. Chem. Eng. 8 (16) (Apr. 2020) 6173–6193, <https://doi.org/10.1021/acssuschemeng.9b07823>.
- [53] M. Chen, M. Li, F. Zhang, X. Hu, Y. Wu, Fast and Efficient CO₂ Absorption in Non-aqueous Tertiary Amines Promoted by Ethylene Glycol, Energy & Fuels 36 (9) (May 2022) 4830–4836, <https://doi.org/10.1021/acs.energyfuels.2c00215>.
- [54] G. Richner, G. Puxty, Assessing the Chemical Speciation during CO₂ Absorption by Aqueous Amines Using In Situ FTIR, Ind. Eng. Chem. Res. 51 (44) (Nov. 2012) 14317–14324, <https://doi.org/10.1021/ie302056f>.
- [55] W. Humphrey, A. Dalke, K. Schulten, VMD: Visual molecular dynamics, J. Mol. Graph. 14 (1) (1996) 33–38, [https://doi.org/10.1016/0263-7855\(96\)00018-5](https://doi.org/10.1016/0263-7855(96)00018-5).
- [56] W. Zhao, et al., Liquid-solid phase-change absorption of acidic gas by polyamine in nonaqueous organic solvent, Fuel 209 (2017) 69–75, <https://doi.org/10.1016/j.fuel.2017.07.081>.
- [57] H.-B. Xie, Y. Zhou, Y. Zhang, J.K. Johnson, Reaction Mechanism of Monoethanolamine with CO₂ in Aqueous Solution from Molecular Modeling, J. Phys. Chem. A 114 (43) (Nov. 2010) 11844–11852, <https://doi.org/10.1021/jp107516k>.